Bolometers and the Big Bang – Detector Arrays for Next-Generation CMB Experiments

Helmuth Spieler

Physics Division
Lawrence Berkeley National Laboratory

Outline:

1. CMB Physics and Experiments
2. Measurement Techniques and Requirements
3. Bolometer Arrays
4. Frequency-Multiplexed Readout
5. System results

More information at www-physics.LBL.gov/~spieler.

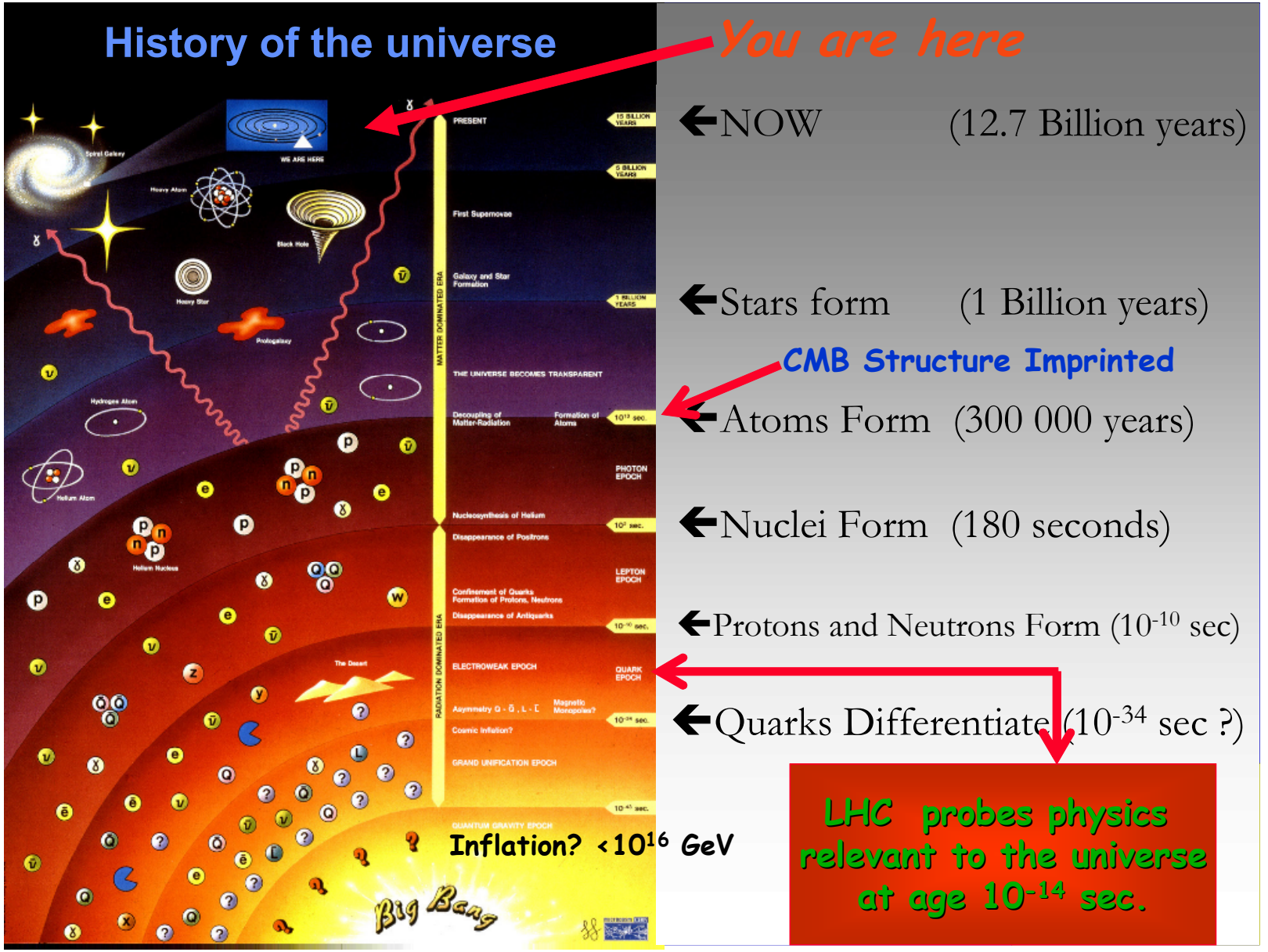
History of the universe
You are here
NOW (12.7 Billion years)
Stars form (1 Billion years)
CMB Structure Imprinted
Atoms Form (300 000 years)
Nuclei Form (180 seconds)
Protons and Neutrons Form (10-10 sec)
Quarks Differentiate (10-34 sec ?)
LHC probes physics relevant to the universe at age 10-14 sec.
Inflation? <10^16 GeV
Big Bang
PRESENT
First Supernovae
Galaxy and Star Formation
THE UNIVERSE BECOMES TRANSPARENT
Decoupling of Matter-Radiation
Formation of Atoms
PHOTON EPOCH
Nucleosynthesis of Helium
Disappearance of Positrons
LEPTON EPOCH
Confinement of Quarks
Formation of Protons, Neutrons
Disappearance of Antiquarks
ELECTROWEAK EPOCH
QUARK EPOCH
Cosmic Inflation?
GRAND UNIFICATION EPOCH
QUANTUM GRAVITY EPOCH
MATTER DOMINATED ERA
RADIATION DOMINATED ERA

CMB has a near perfect black body spectrum (T = 2.7K)
– measurements within 1% of theoretical spectrum

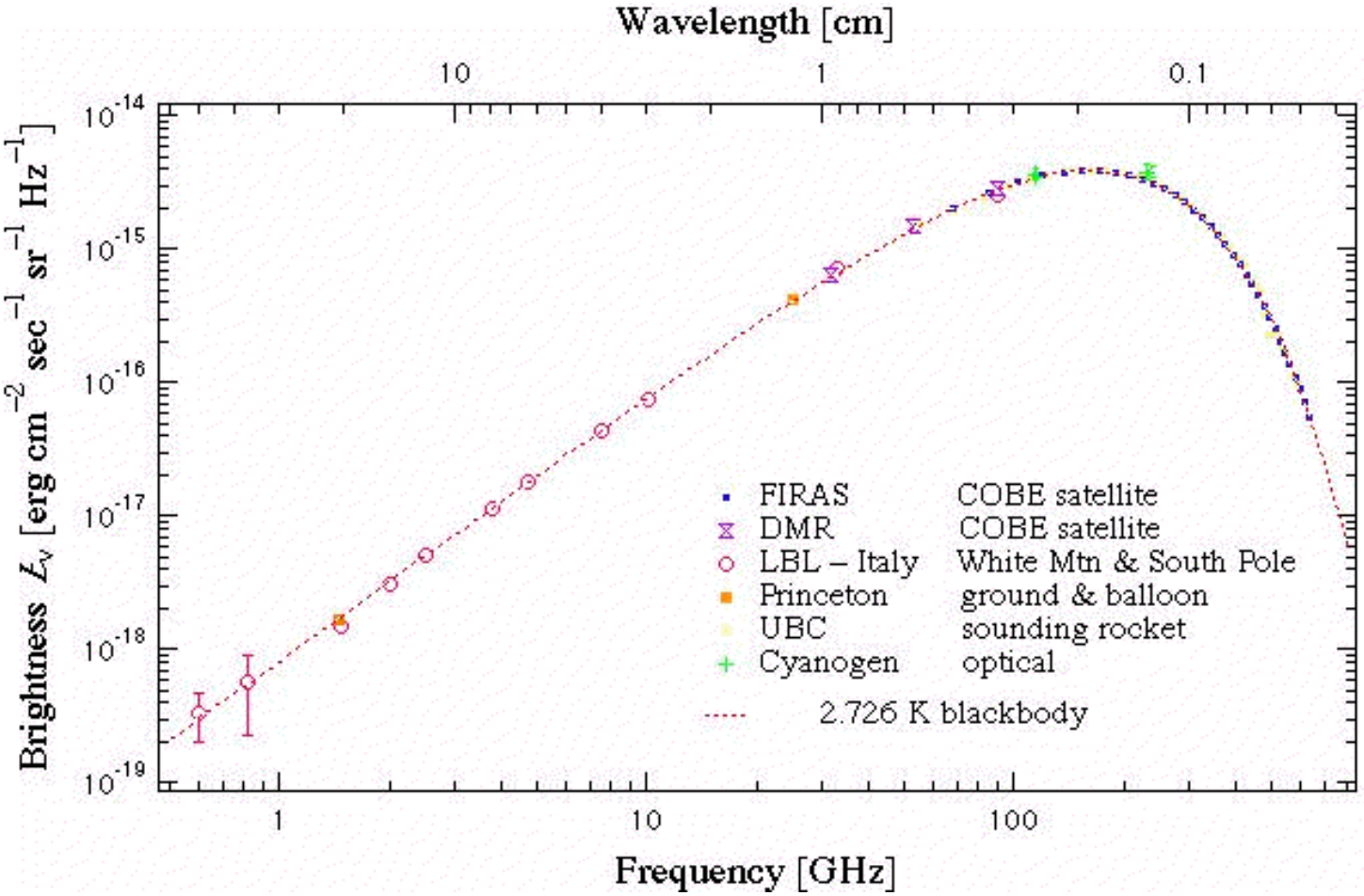

CMB very well understood – has provided precision data on key cosmological parameters.

Map Temperature of Sky:

Data from WMAP

Temperature anisotropy ~10^{-5}

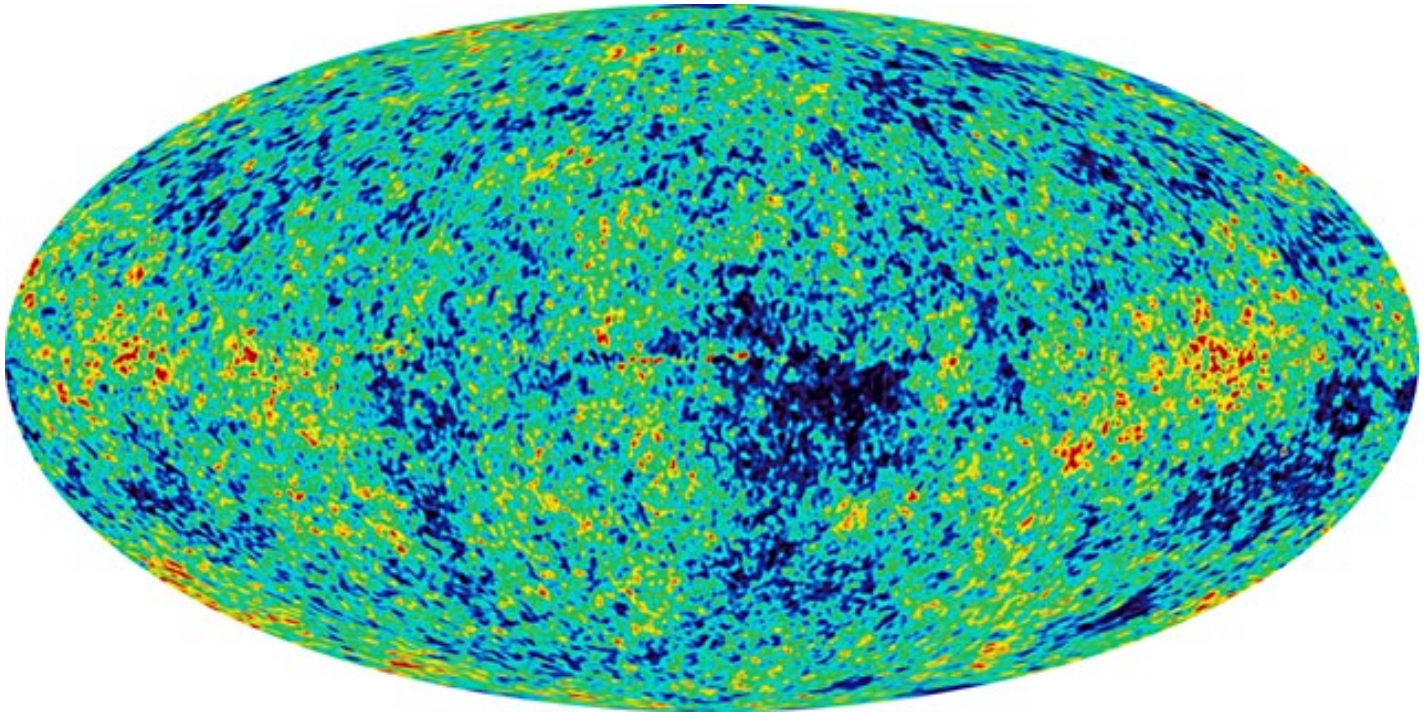

Multipole expansion of spatial distribution – determine angular scales

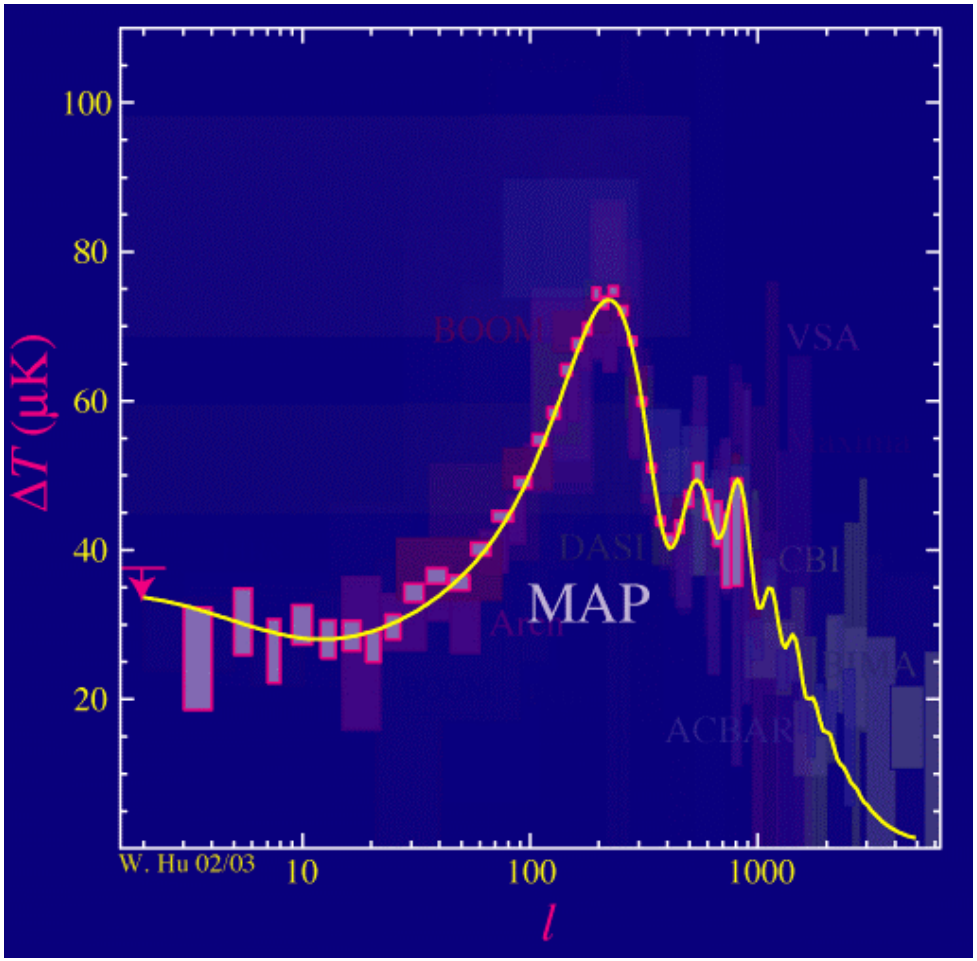

angular resolution $\Delta\Theta \approx 180/\ l$

Angular structure depends on cosmological parameters

For example, geometry:
dominant angular scale ~1°

$\Rightarrow$ universe is flat

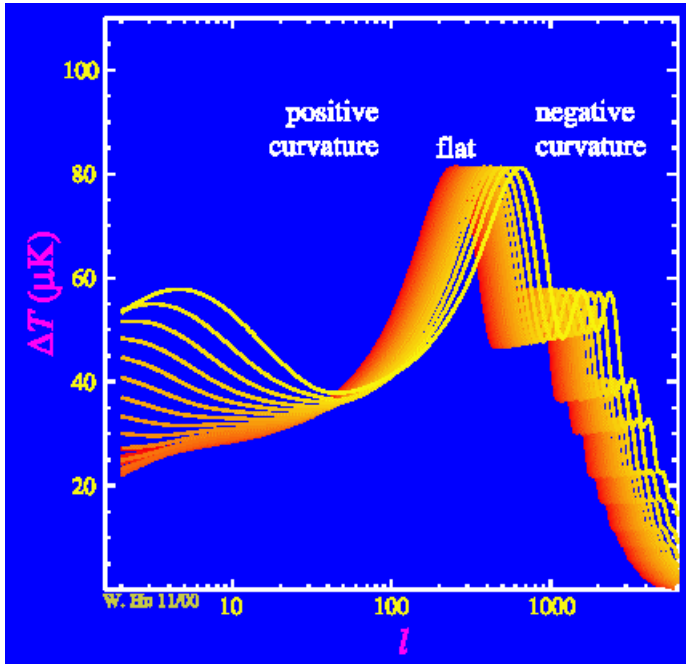

Analyzing the power spectrum:

Normalization set by the total amount of matter $\Omega_M = \Omega_b + \Omega_{CDM}$

Position of 1st peak: geometry of universe

$l > 200$	$\Omega_0 > 1$	pos. curv.
$l \approx 200$	$\Omega_0 = 1$	flat
$l < 200$	$\Omega_0 < 1$	neg. curv.

Ratio of 1st to 2nd peak: amount of baryonic matter

3rd peak > 2nd peak: presence of cold dark matter

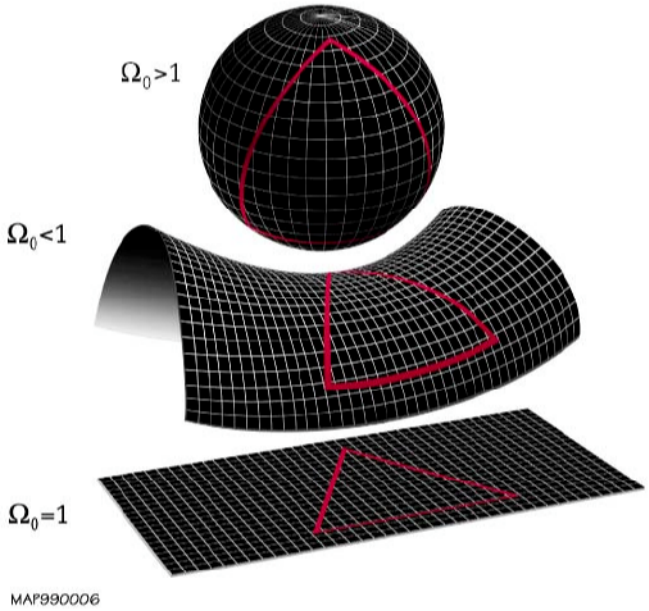

- CMB measurements provide constraints on fundamental cosmological parameters
- CMB spatial distribution largely unaffected since 300k yrs after Big Bang
- Supernova and CMB data *together* give best constraints on mass and energy density of the universe
- Also consistent with Ω_m from Large Scale Structure data

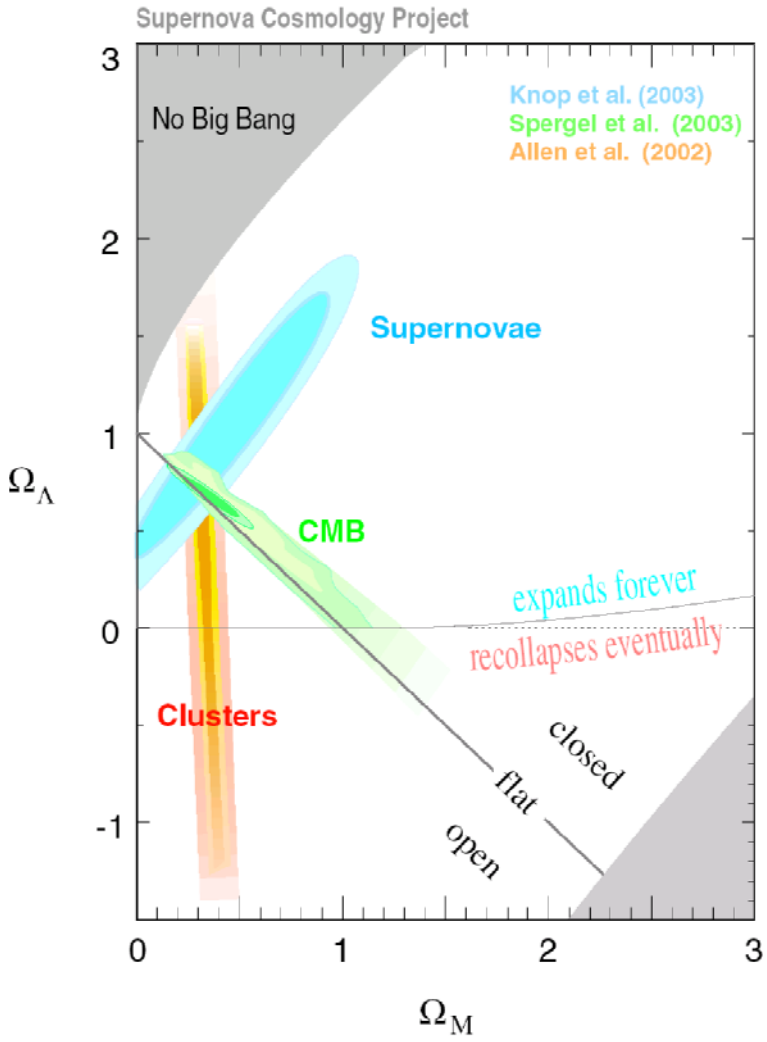

Cosmology relies on combined data from different techniques

Today we use CMB as a tool:

1. Map large-scale structure:
   use Sunyaev-Zel'dovich Effect in galaxy cluster search $\Rightarrow$ w, Ω_m

Inverse Compton scattering: Hot gas bound to clusters of galaxies scatters CMB

$\Rightarrow$ distorts black-body spectrum – shifts to higher frequencies:

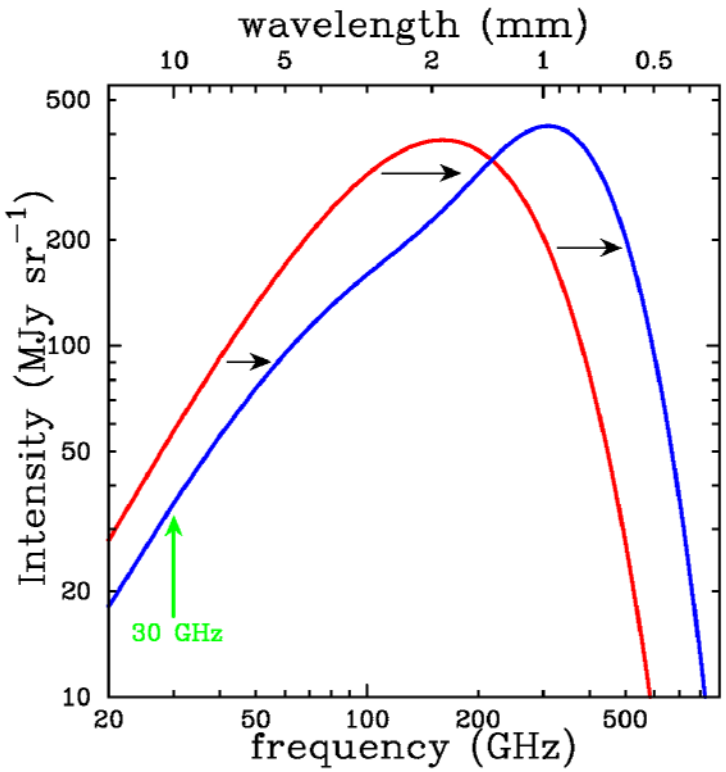

Clusters appear as dark spots in CMB sky

Galaxy cluster searches

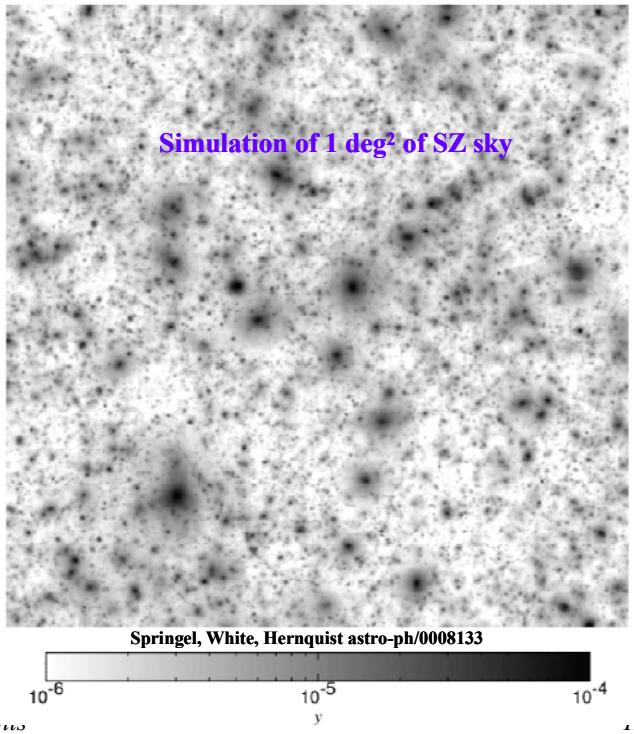

SZ signal independent of redshift z

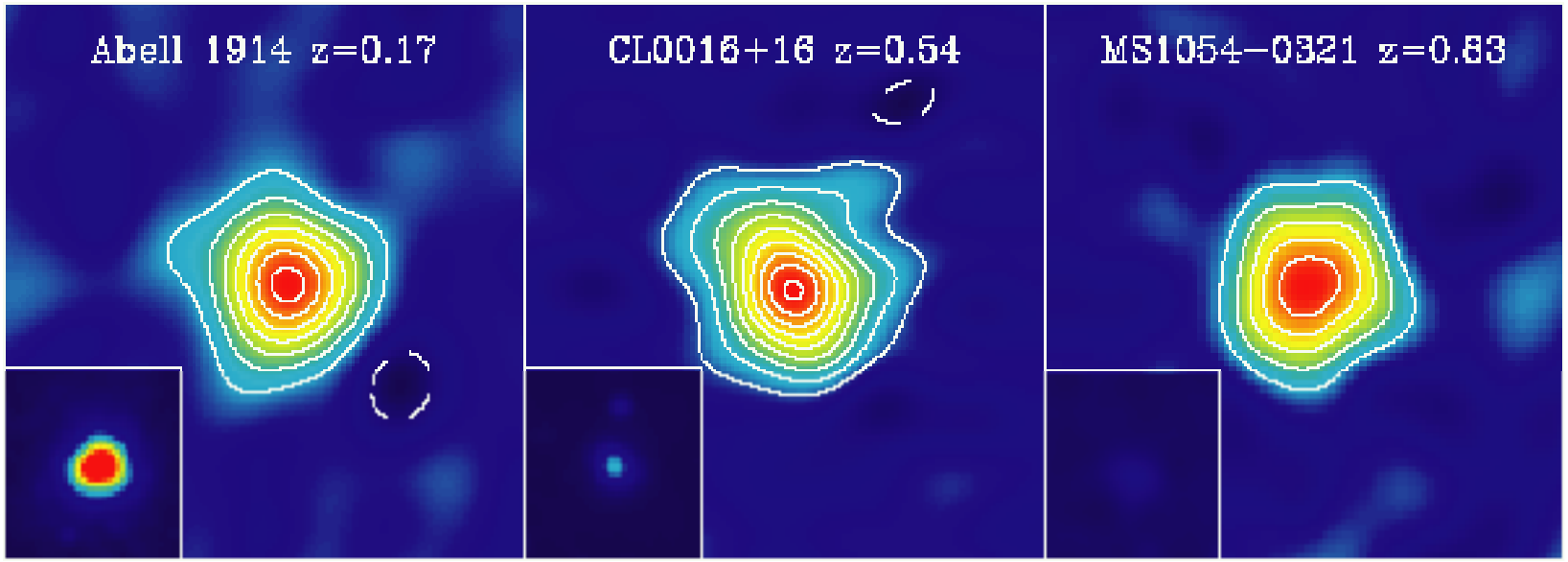

(Holzapfel et al.)

In contrast to x-rays (insets), SZ surface brightness is independent of redshift, so clusters can be seen at any distance.

However, optical data needed to determine redshift.

Emerging technique that requires greatly improved arrays.

Cluster densities at z > 1 sensitive to cosmological parameters

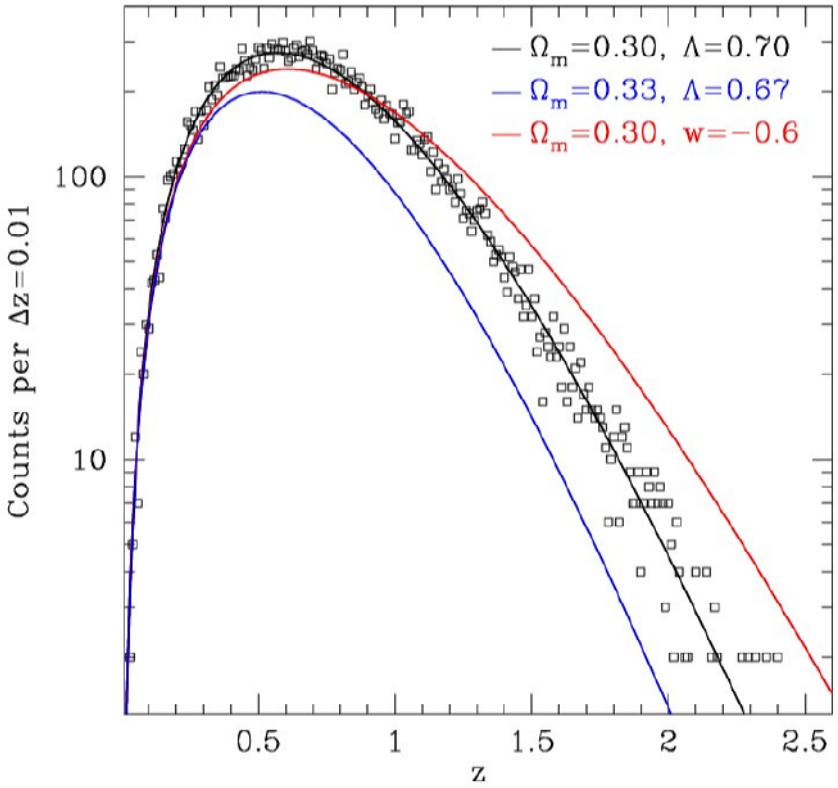

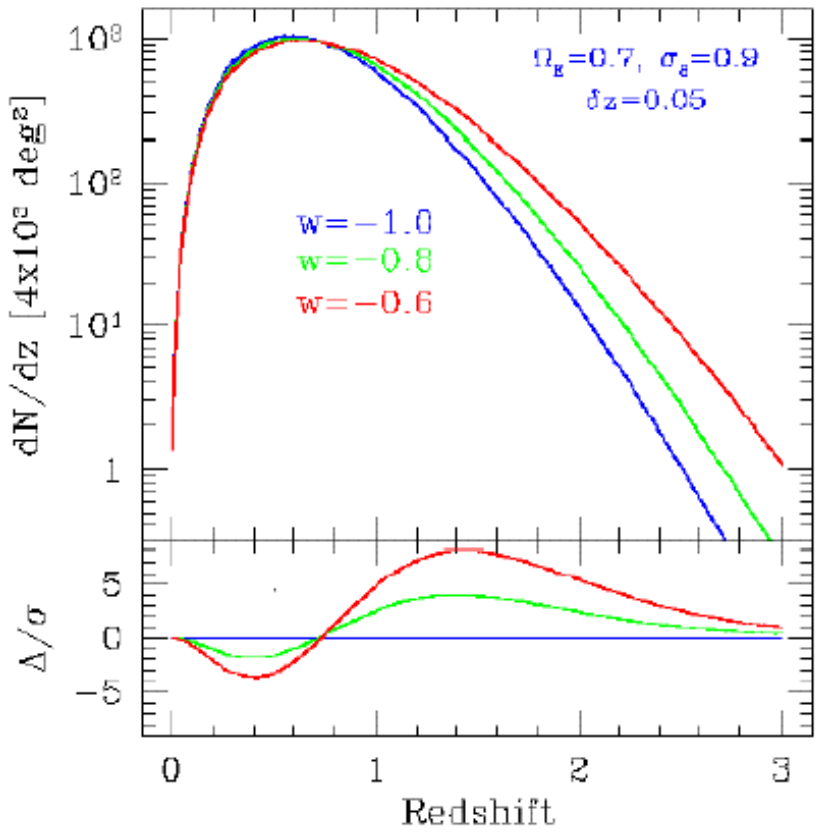

2. CMB Polarization

Thomson scattering ⇒ Polarization

If CMB were perfectly isotropic, all polarizations would occur equally

⇒ no net polarization.

However, CMB is anisotropic:

Quadrupole anisotropy yields net polarization.

⇒ patterns with no preferential handedness in polarization field (“E modes”)

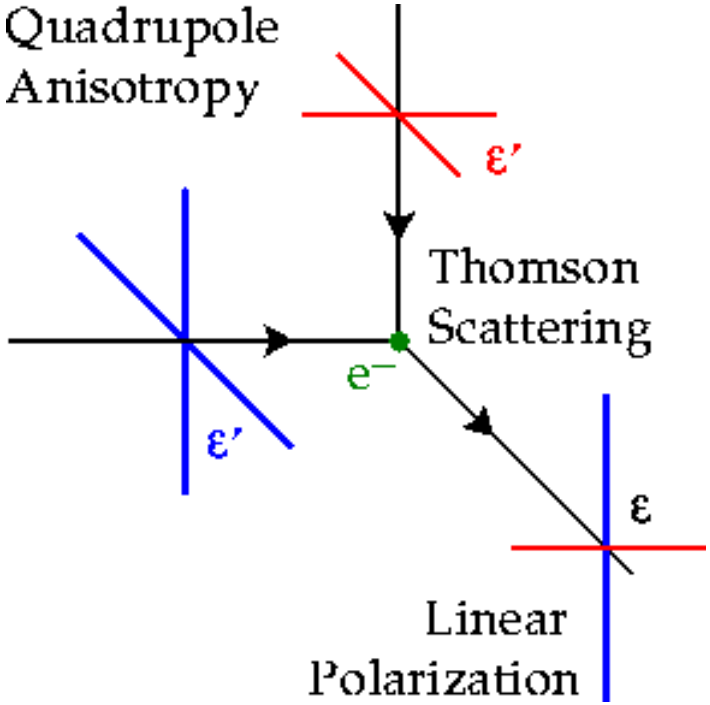

CMB Polarization allows us to look beyond the time of last scattering:

Gravity waves emitted during inflation (~10^{-38} s after Big Bang) interact with matter and leave imprint on surface of last scattering.

CMB temperature is image of matter distribution.

Gravity waves: tensor interaction ⇒ net curl in polarization field (“B-modes”)
(“smoking gun” of inflation)

Gravity waves generate B-modes: Polarization field has net “handedness”.

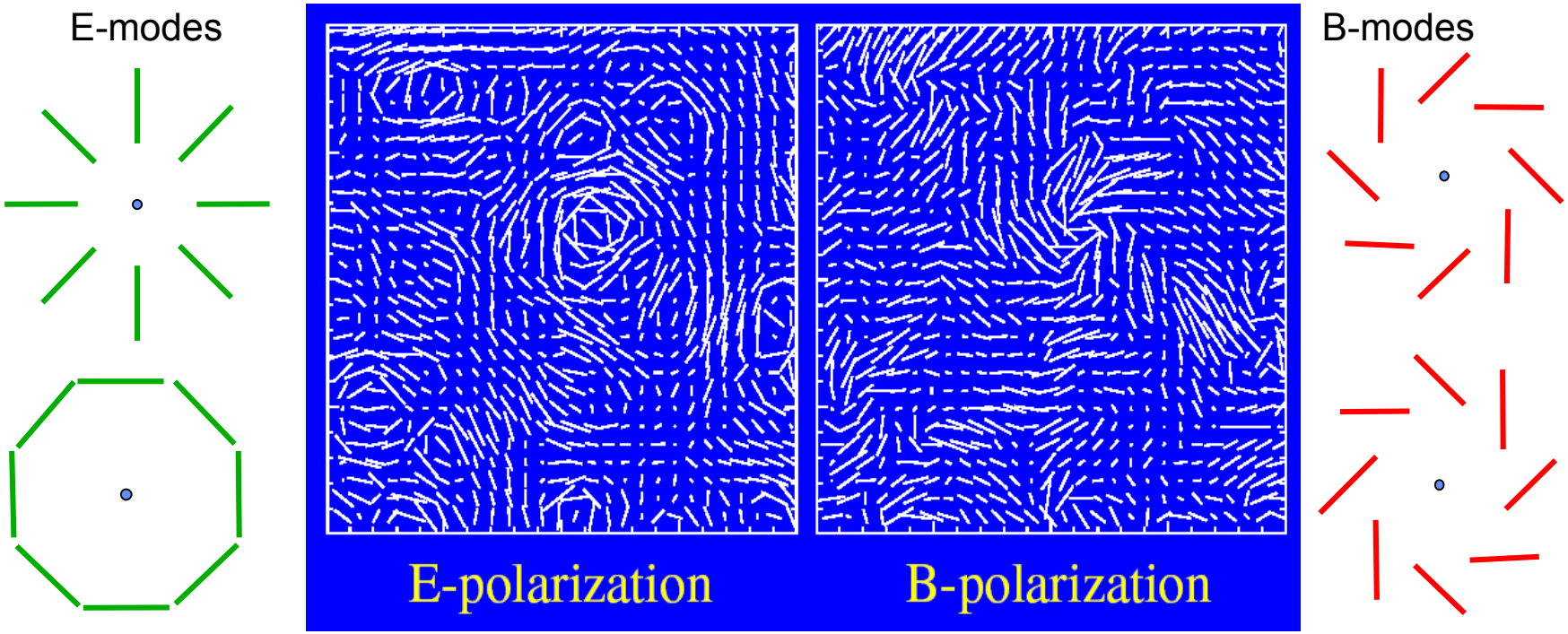

Wayne Hu

Density fluctuations give scalar perturbations ⇒ E-modes

Gravity waves give tensor perturbations ⇒ B-modes

E-mode polarization detected
(Carlstrom et al., DASI)

Challenge:

Detection and characterization of B-modes

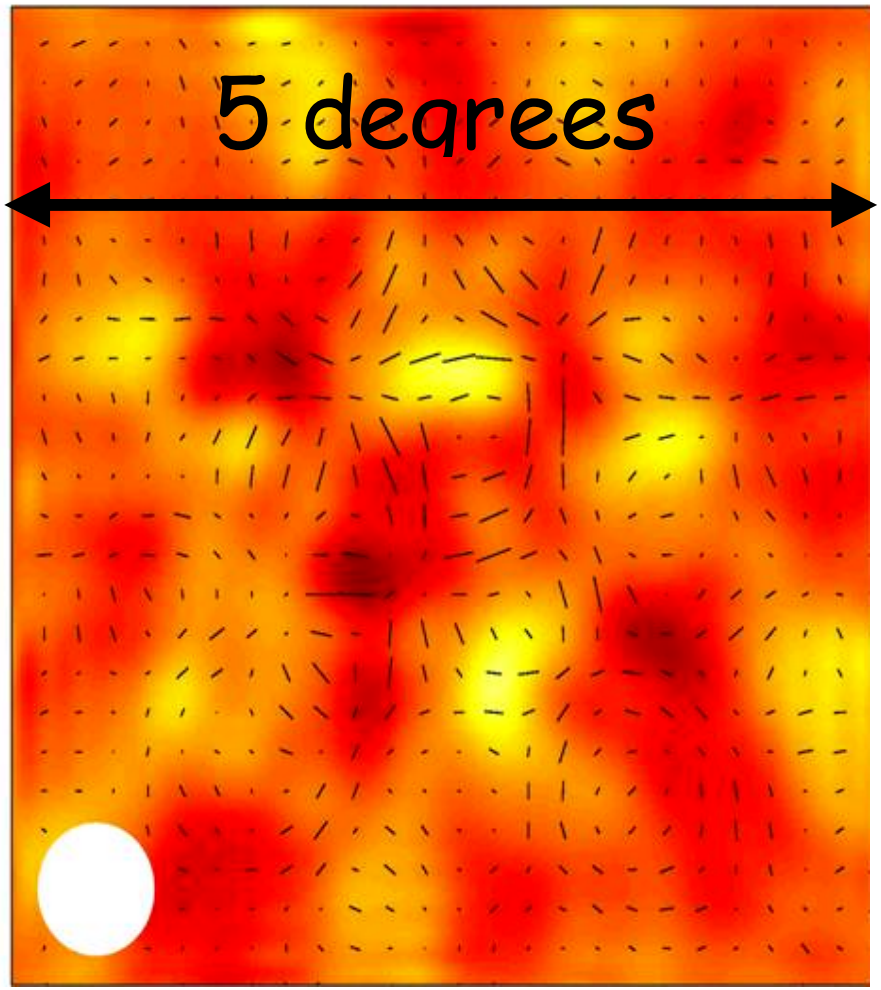

Required Sensitivity

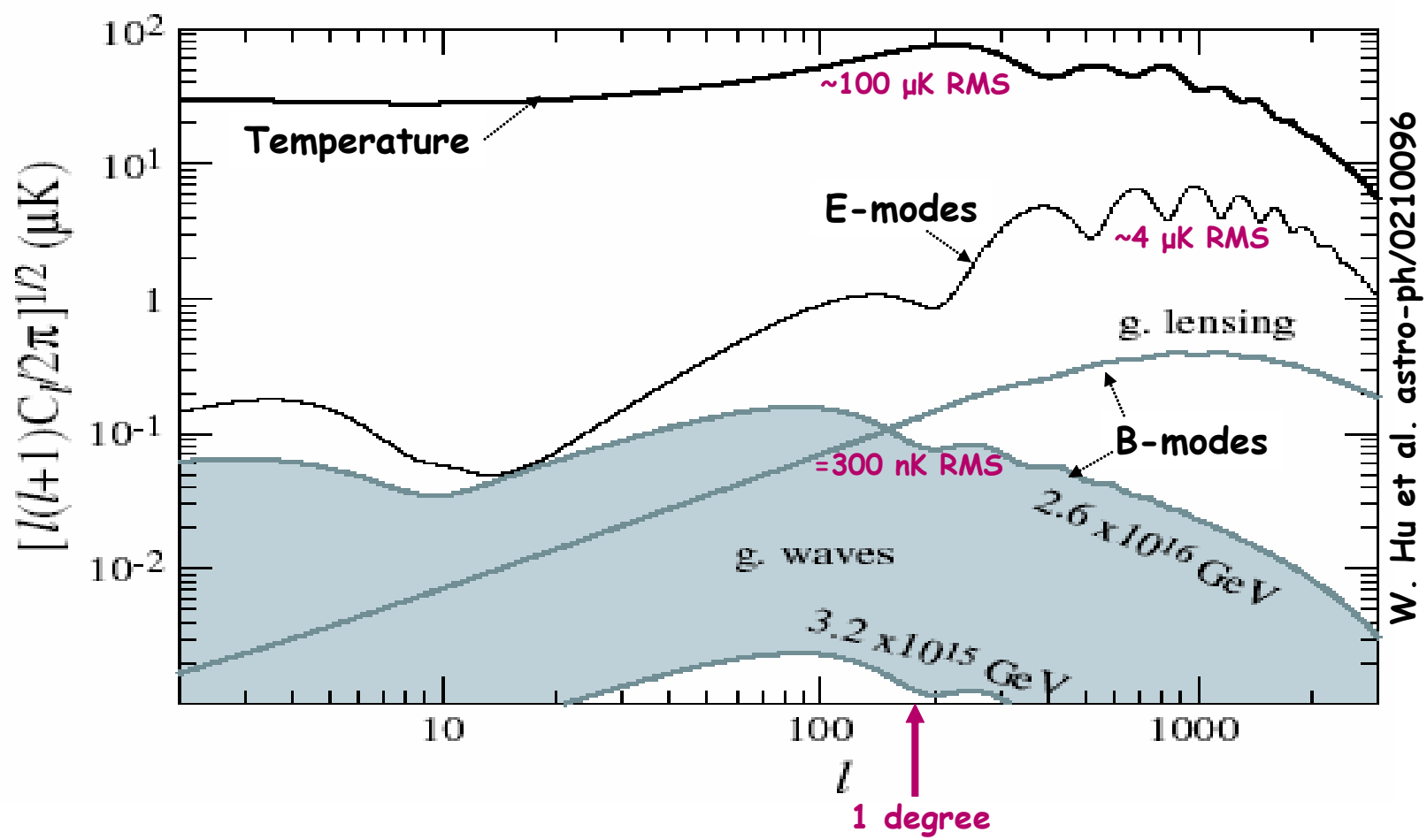

Magnitude of gravity wave signal set by **energy scale of inflation**

B-modes are also generated by weak lensing of E-mode polarization

Gravity wave signature and lensing have different angular scales

Requires 3m reflector to provide angular resolution.

DETECTED SIGNAL

- View region of sky with temperature T (CMB: $T \approx$ 3K)
- Measured signal proportional to kTB (B = bandwidth)

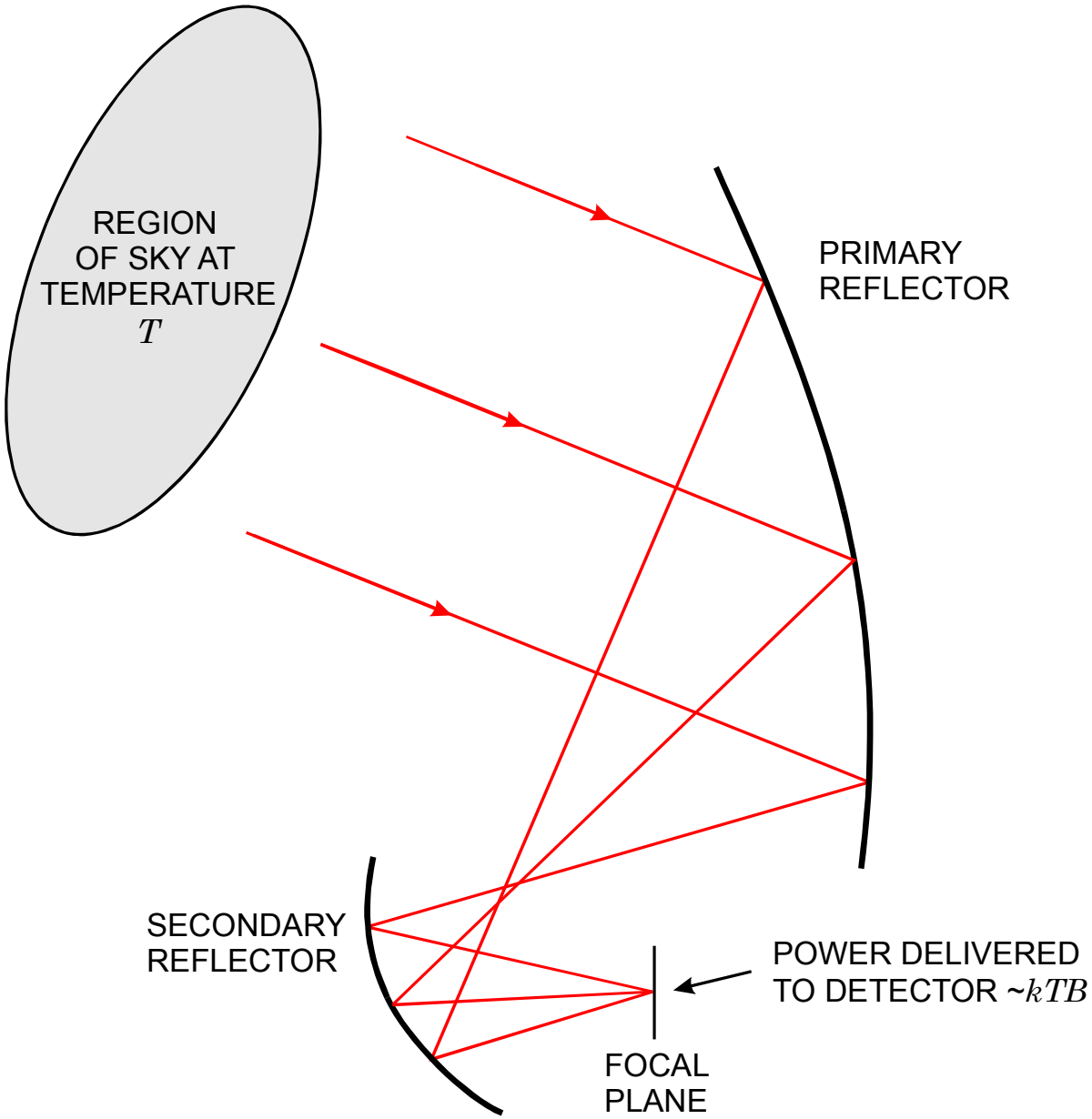

Example Optics and Focal Plane (South Pole Telescope)

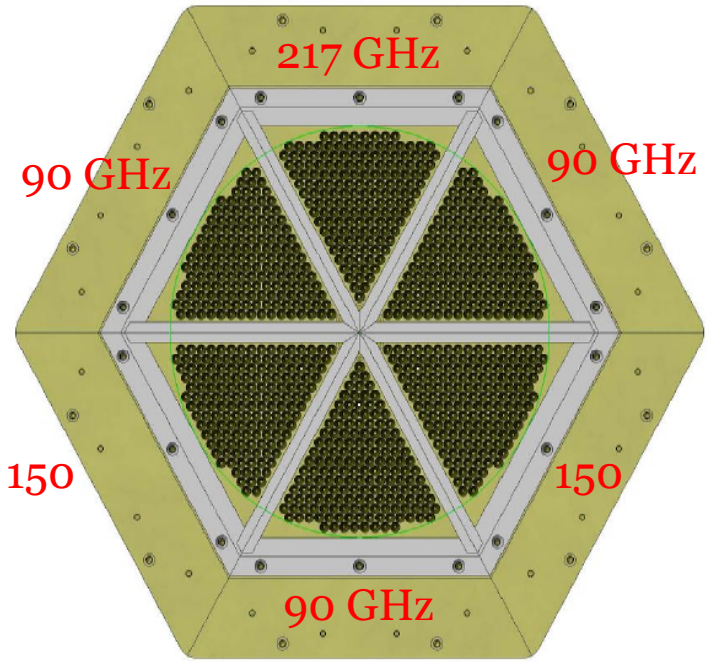

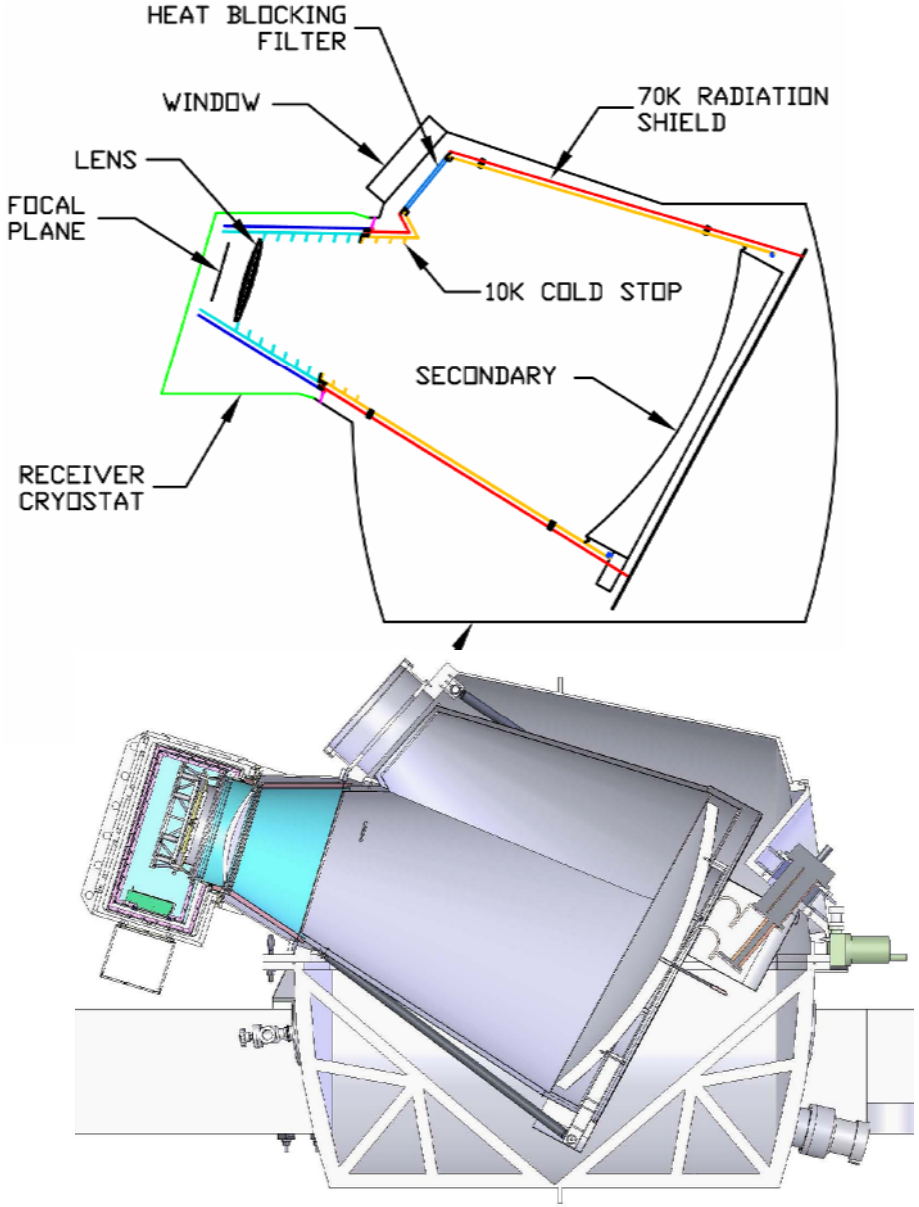

COUPLING TO BOLOMETER

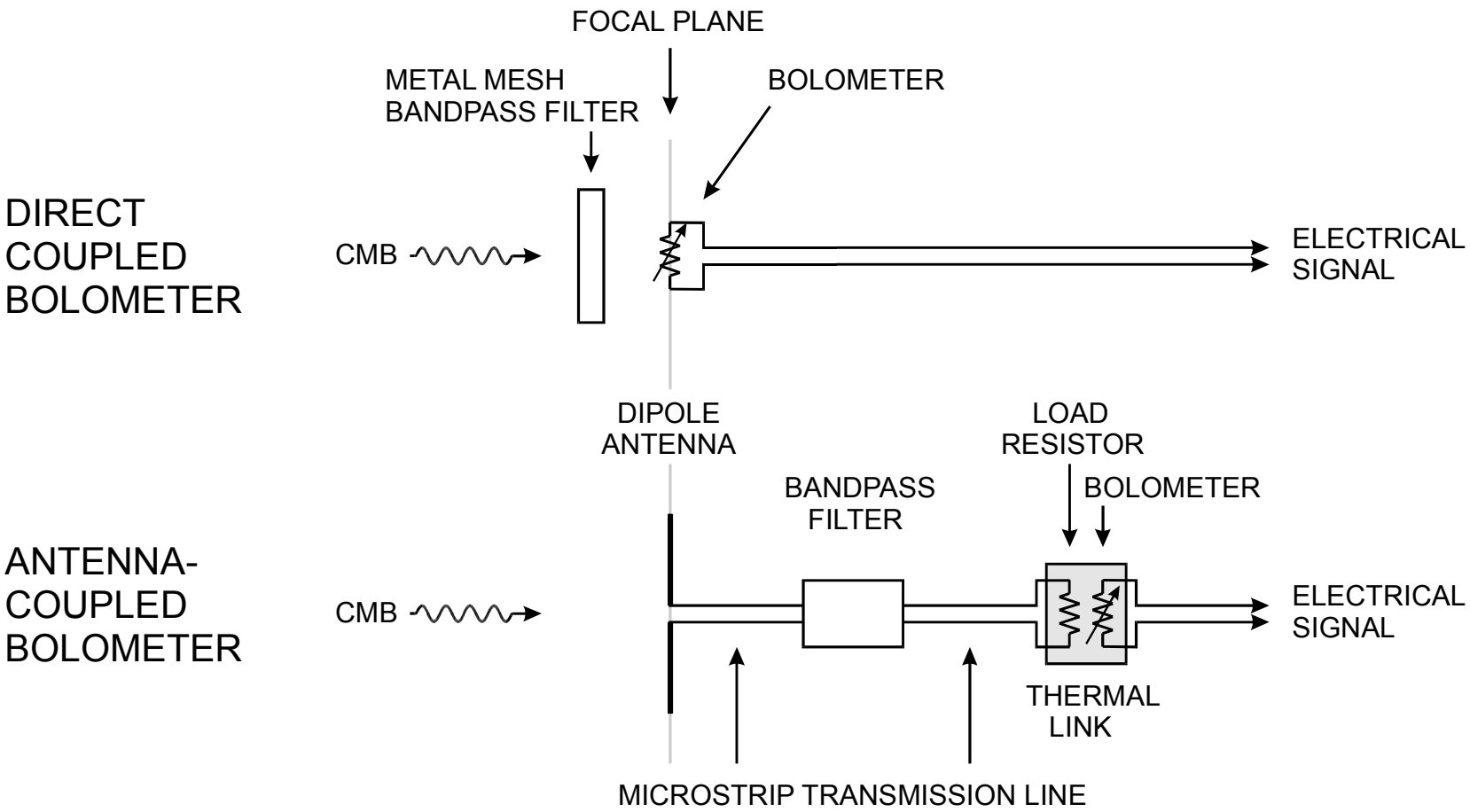

Antenna-coupling provides inherent polarization sensitivity.

Signal Spectrum in Galaxy Cluster Search

Antenna beam width: 1’ FWHM Scan speed: 10’/s

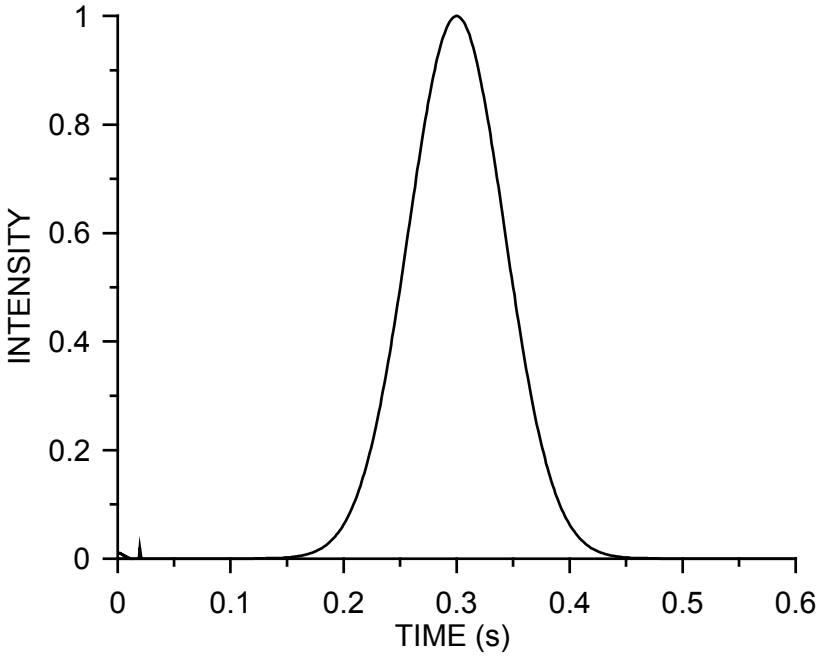

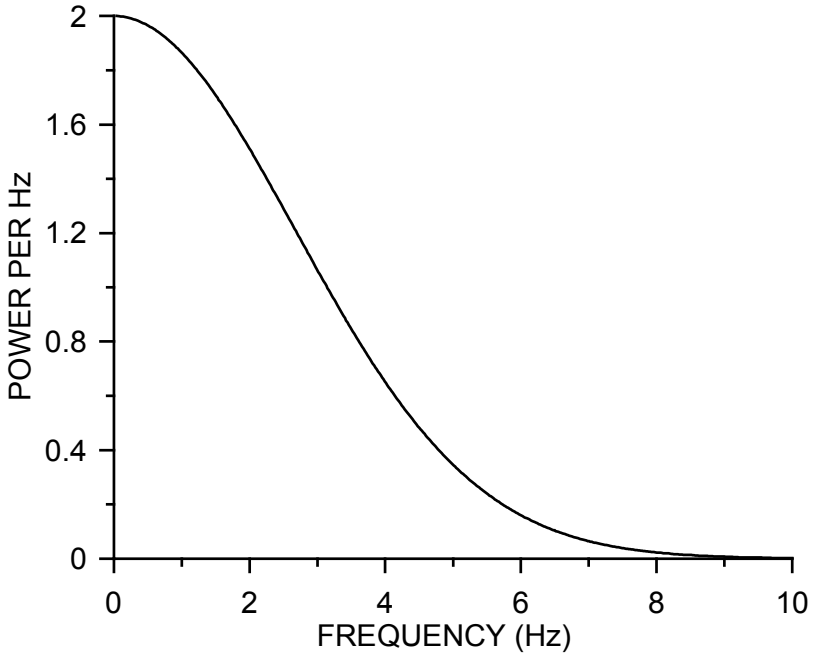

(W. Lu, CWRU)

⇒ Maintain Gain Stability + Noise Level down to ~0.1 Hz

Some Next Generation Experiments:

1. Cluster Searches:

a) APEX-SZ

UCB, LBNL, MPIfR, Colorado, McGill

12 m on-axis telescope
(ALMA prototype) on
Atacama Plateau, Chile, 5000m

~300 pixels

Shared with many other
experiments, so CMB observing
time limited to few weeks

APEX-SZ first light Dec 2005

b) South Pole Telescope

Univ. Chicago, UCB, LBNL, CWRU, CfA, Univ. Colorado, McGill, Univ. Illinois

10 m off-axis telescope

Installation: 2006-2007

~1000 pixels, dedicated to CMB measurements

Optical followup with DES

Test assembly in Texas (August 2006)

January 3, 2007 at South Pole

SPT final configuration with ground shield (Jan 2008)

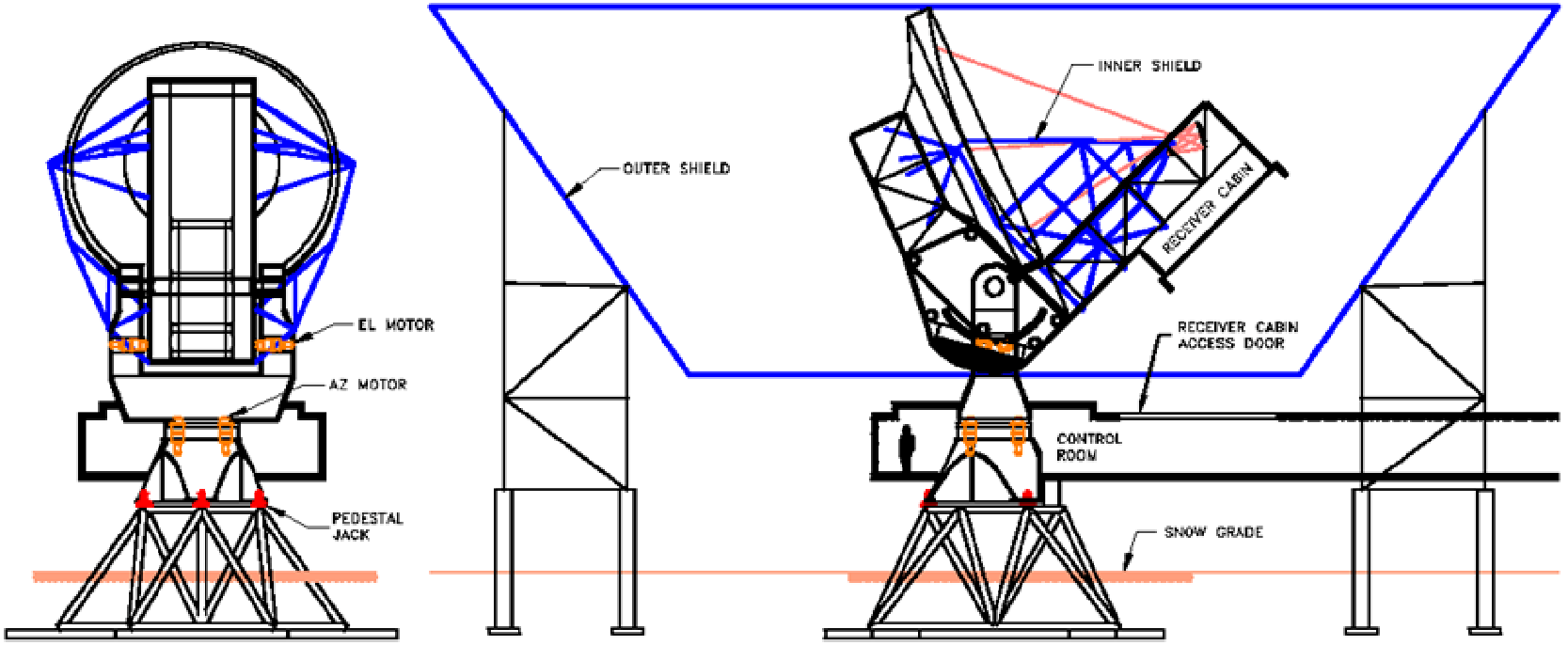

2. Polarization & Inflation: PolarBear (UCB, LBNL, UCSD, Colorado, McGill)

Reviewed by SAGENAP, proposal to NSF

Atacama plateau (Chilean Andes, 5000 m altitude)

~1000 dual polarization pixels

3m telescope: angular resolution to separate gravitational from lensing B-modes

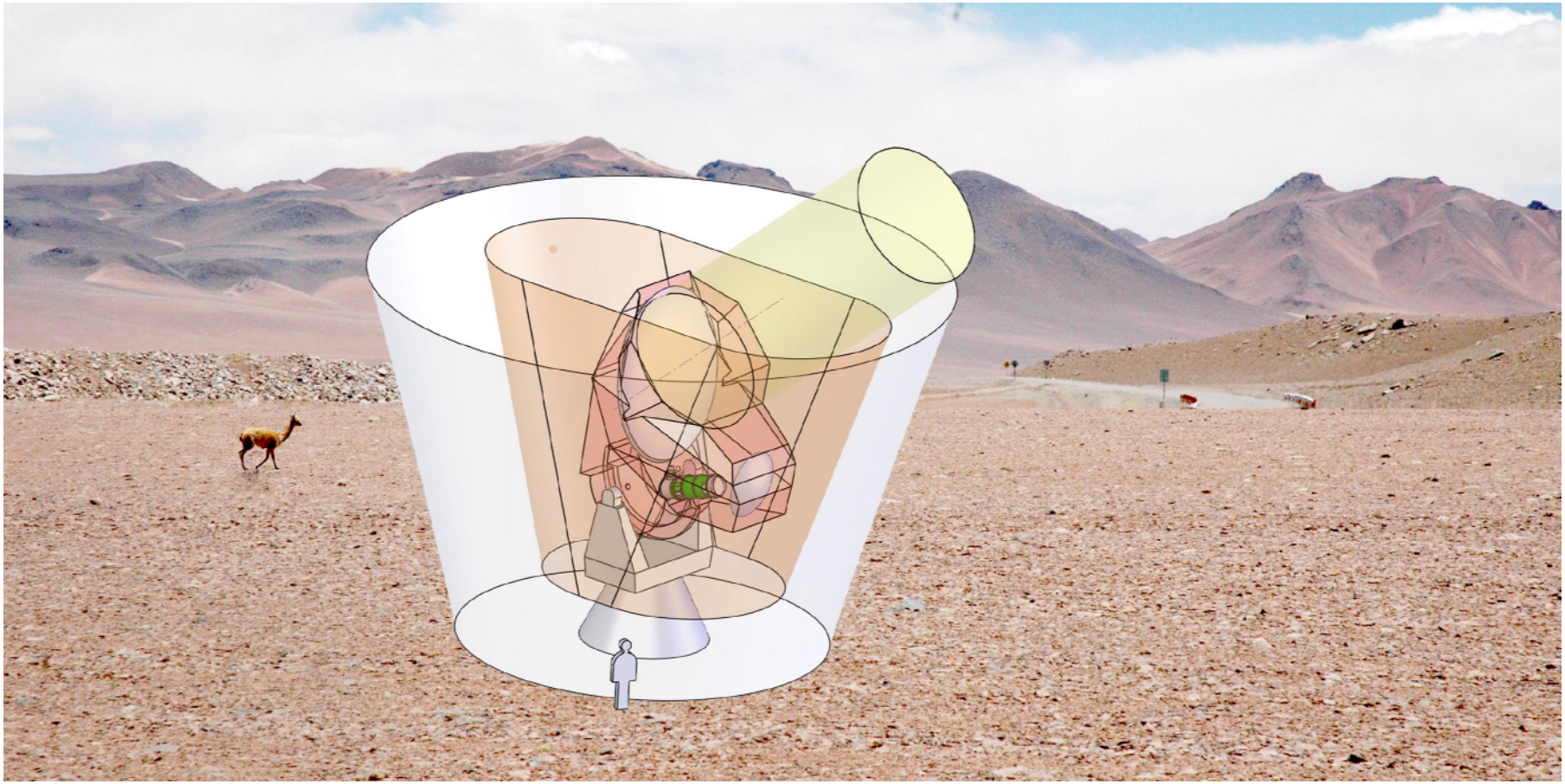

PolarBear designed from ground up to optimize polarization measurements

⇒ Minimize cross-polarization and instrumental polarization
Sensitivity and resolution to separate E and B modes

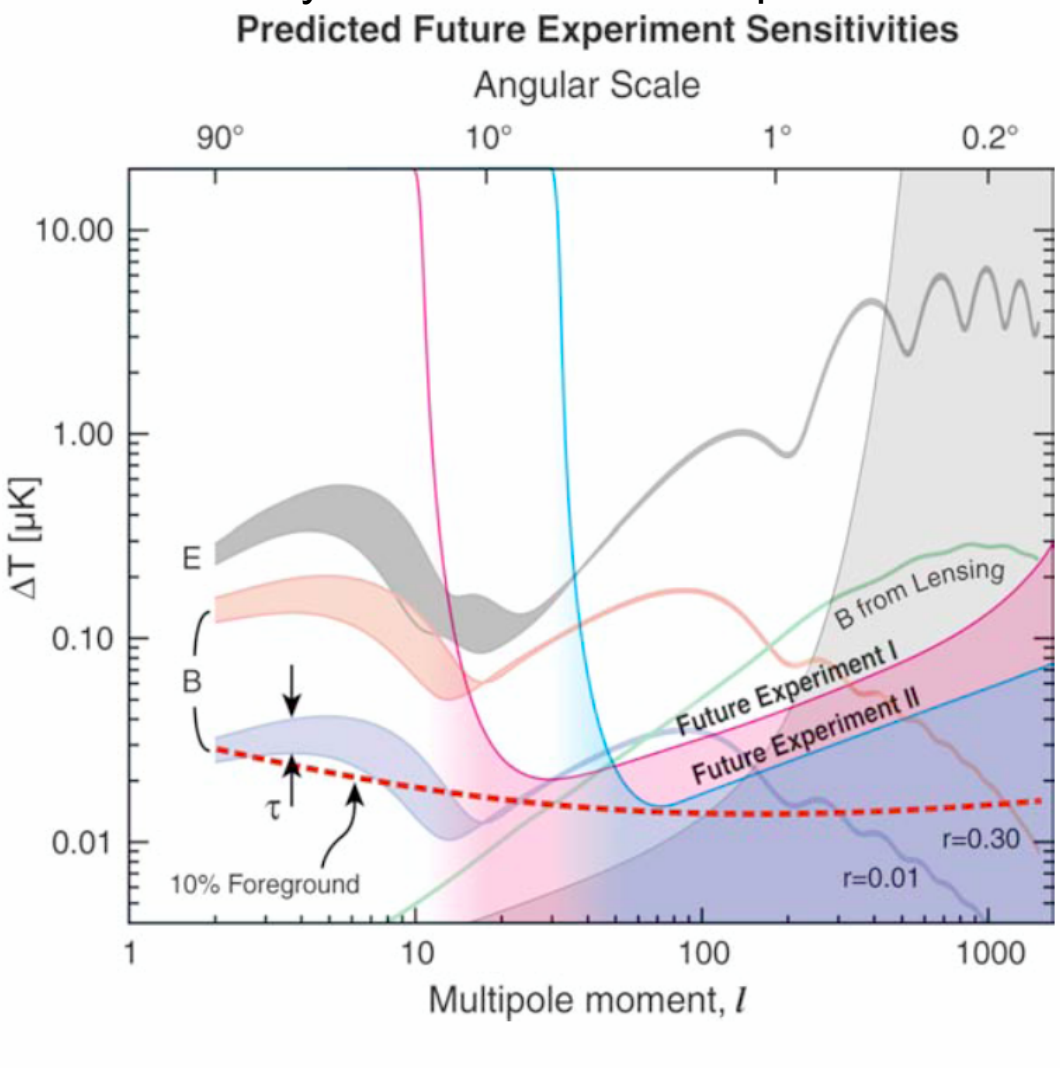

PolarBear performance similar to Experiment I

from Interagency Task Force on CMB Research ("Weiss Committee")

All of these experiments require a major step up in sensitivity

Bolometers today are so sensitive that we are limited by the shot noise of the CMB photons

Increase sensitivity by

performing many measurements simultaneously

$\Rightarrow$ bolometer arrays (100s to 1000s)

extending observation time

$\Rightarrow$ ground-based experiments

eventually space-based

Bolometer array technology:

Wafer-scale monolithic fabrication ("radiometer on a chip")

Cold multiplexing on 0.25K stage (reduce heat leaks through wiring)

Cryogen free system: pulse tube cooler + ^{4}He/^{3}He/^{3}He sorption fridge (remote operation with minimal on-site staff)

Berkeley Bolometer Group

William Holzapfel (UCB)
Adrian Lee (LBNL,UCB)
Paul Richards (UCB)
Helmuth Spieler (LBNL)

John Clarke (LBNL,UCB) SQUIDs

Greg Engargiola (UCB RAL)
John Joseph (Eng. Div. LBNL)
Chinh Vu (Eng. Div. LBNL)

Brad Benford (UCB)
H.-M. "Sherry" Cho (UCB)
Matt Dobbs (LBNL
– now McGill Univ.)
Nils Halverson (UCB
– now Univ. Colorado)
Huan Tran (UCB SSL)

+ 15 graduate students

Funding: NSF, NASA, DoE

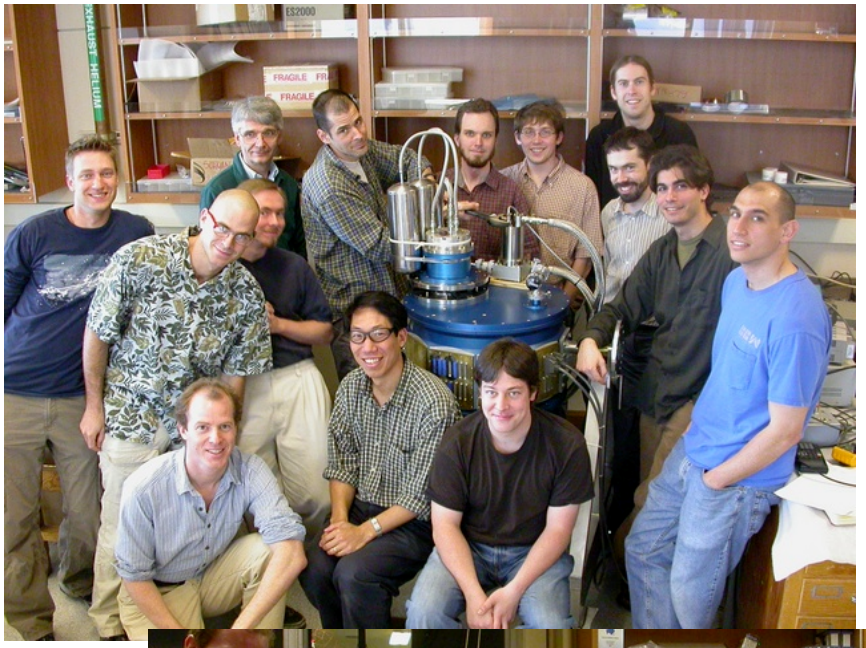

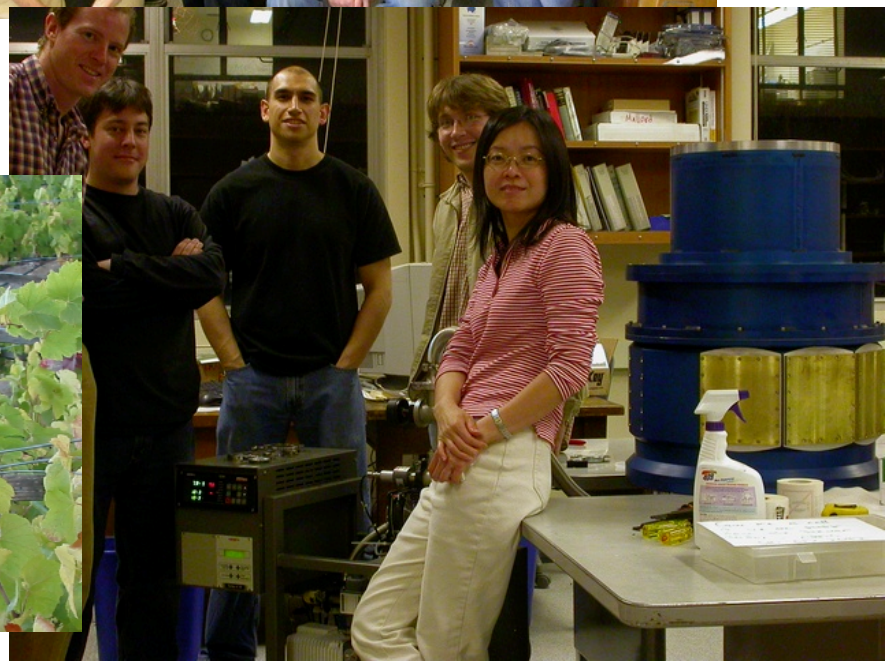

Bolometers

Superconducting transition edge sensors:

- Bias thin film superconductor at transition from super- to normal conducting

⇒ Large change in resistance with absorbed power

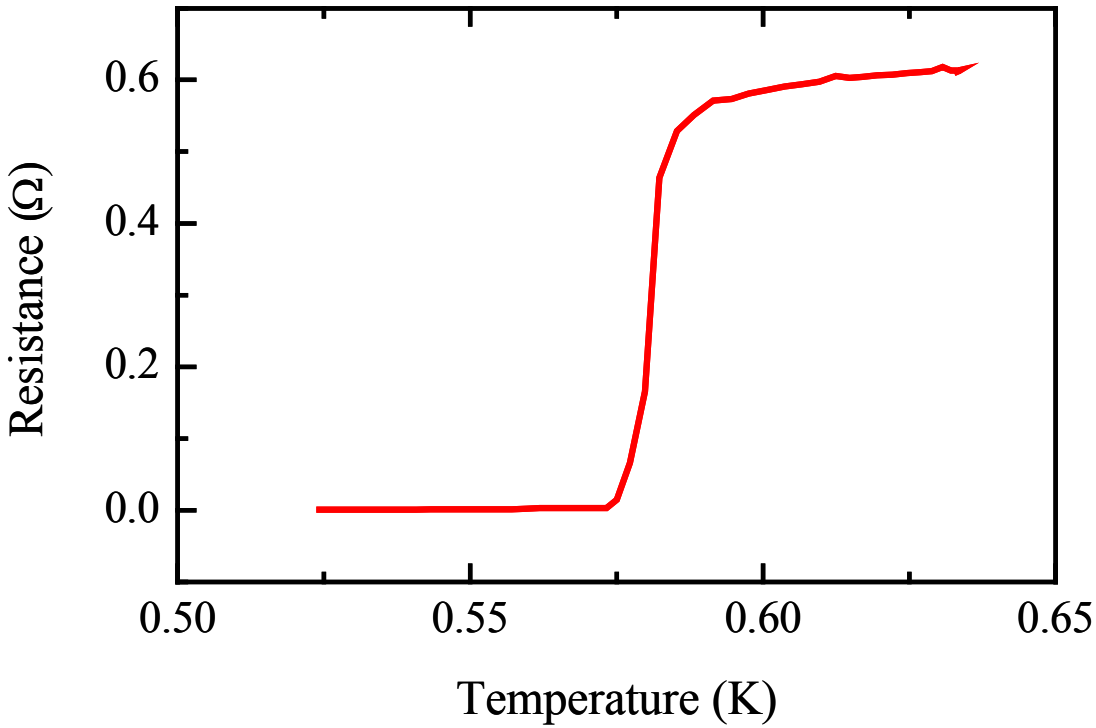

- Thin bi-layers (e.g. Al – Ti) allow tuning of transition temperature

Why Bolometers?

Amplifiers (phase coherent systems) subject to quantum noise limit.

Minimum spectral noise power density: $\frac{dP_n}{d\omega} = \hbar\omega$

Follows from uncertainty principle.

(H.A. Haus and J.A. Mullen, Phys. Rev. 128 (1962) 2407-2413)

For a simple derivation see Spieler, *Semiconductor Detector Systems*, pp. 132-133

Bolometers do not preserve phase, so not subject to quantum noise limit.

Thermal Detectors

Basic principle:

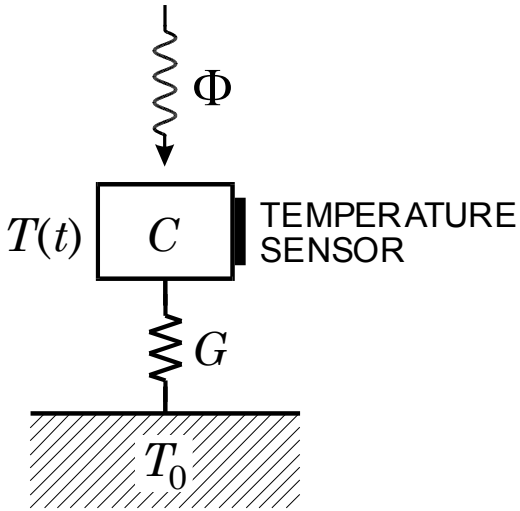

Assume thermal equilibrium:

If all absorbed Energy $E = \Phi \Delta t$ is converted into phonons, the temperature of the sample will increase by

$$\Delta T = \frac{E}{C} ,$$

where C the heat capacity of the sample (specific heat x mass).

After absorption of an energy packet E the heat flows through the thermal conductance G and the bolometer temperature decays as

$$T - T_0 = \frac{E}{C} e^{-t/\tau}$$

with the thermal time constant

$$\tau = \frac{C}{G} ,$$

analogous to a capacitor discharged through a resistance.

Voltage-Biased Transition-Edge Sensors

Required power is of order pW, i.e. voltage of order μV
current of order μA

Simplest to bias device with a constant current and measure change in voltage

Problem: power dissipated in sensor $P = I^2 R$

Increasing R $\Rightarrow$ Increasing P $\Rightarrow$ Increasing R $\Rightarrow$ Increasing P

$\Rightarrow$ thermal runaway

When biased with a constant voltage $P = \frac{V_b^2}{R}$

Increasing R $\Rightarrow$ Decreasing P $\Rightarrow$ Decreasing T $\Rightarrow$ Decreasing R

$\Rightarrow$ **negative feedback**

stabilizes operating point

Analogous to op-amp: Bolometer time constant corresponds to amplifier cutoff frequency.
Subject to constraints of feedback theory!

- Operate with constant voltage bias

$\Rightarrow$ Electrothermal negative feedback

$\Rightarrow$ Stabilize operating point + predictable response

$\Rightarrow$ "Constant power operation":
Change in absorbed power is balanced by change in electrical power: $\Delta I / \Delta P = 1 / V_{bias}$

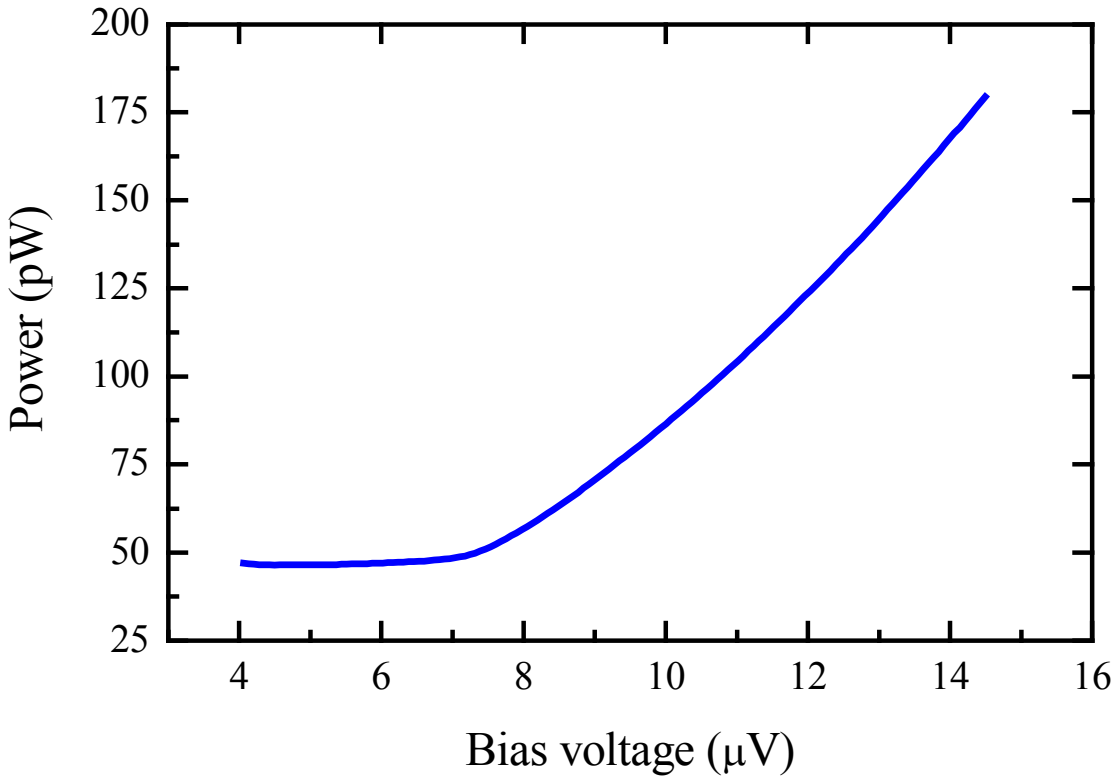

DIRECT COUPLED BOLOMETERS

APEX Focal Plane (Jared Mehl)

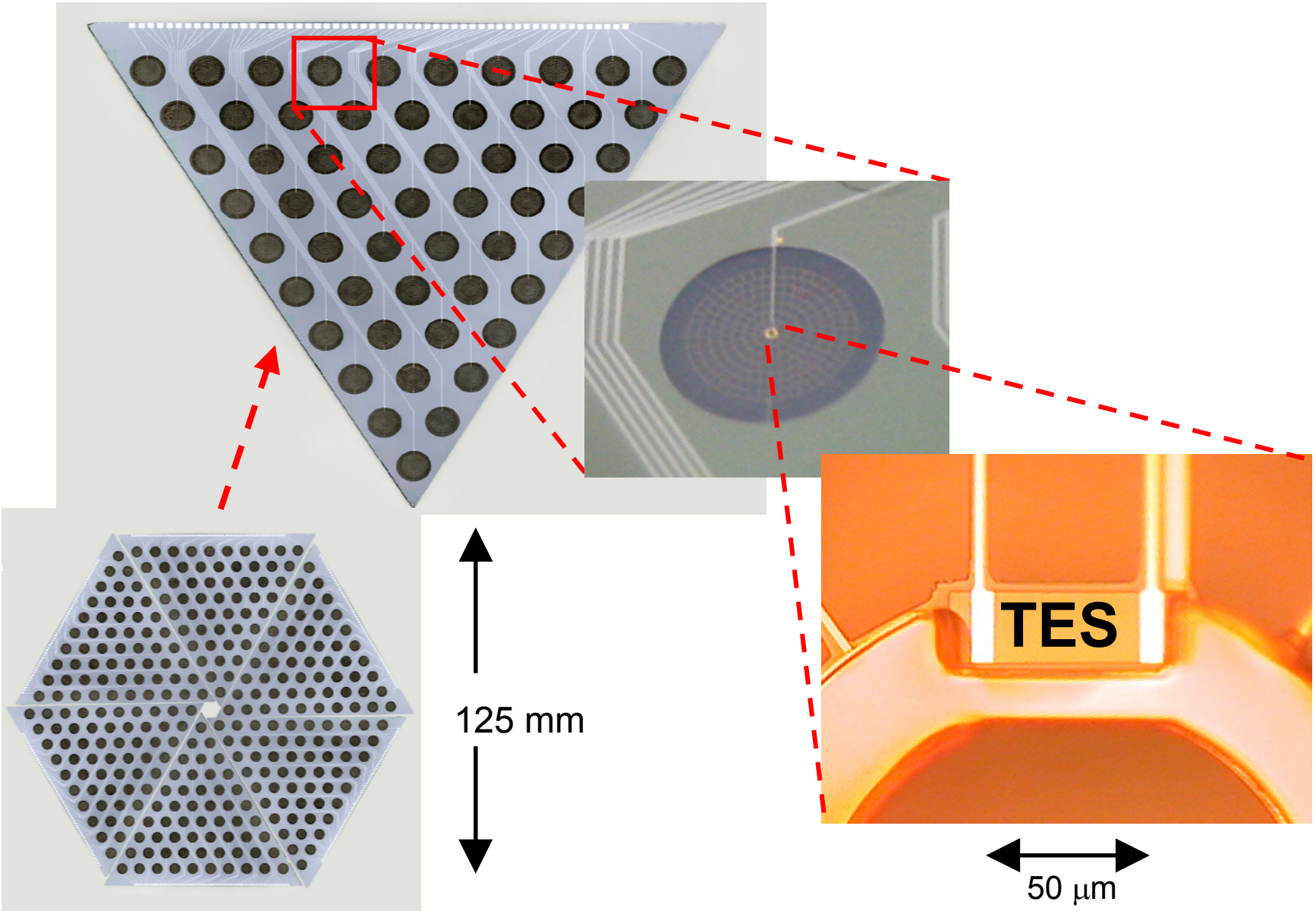

Close-up of spiderweb bolometer

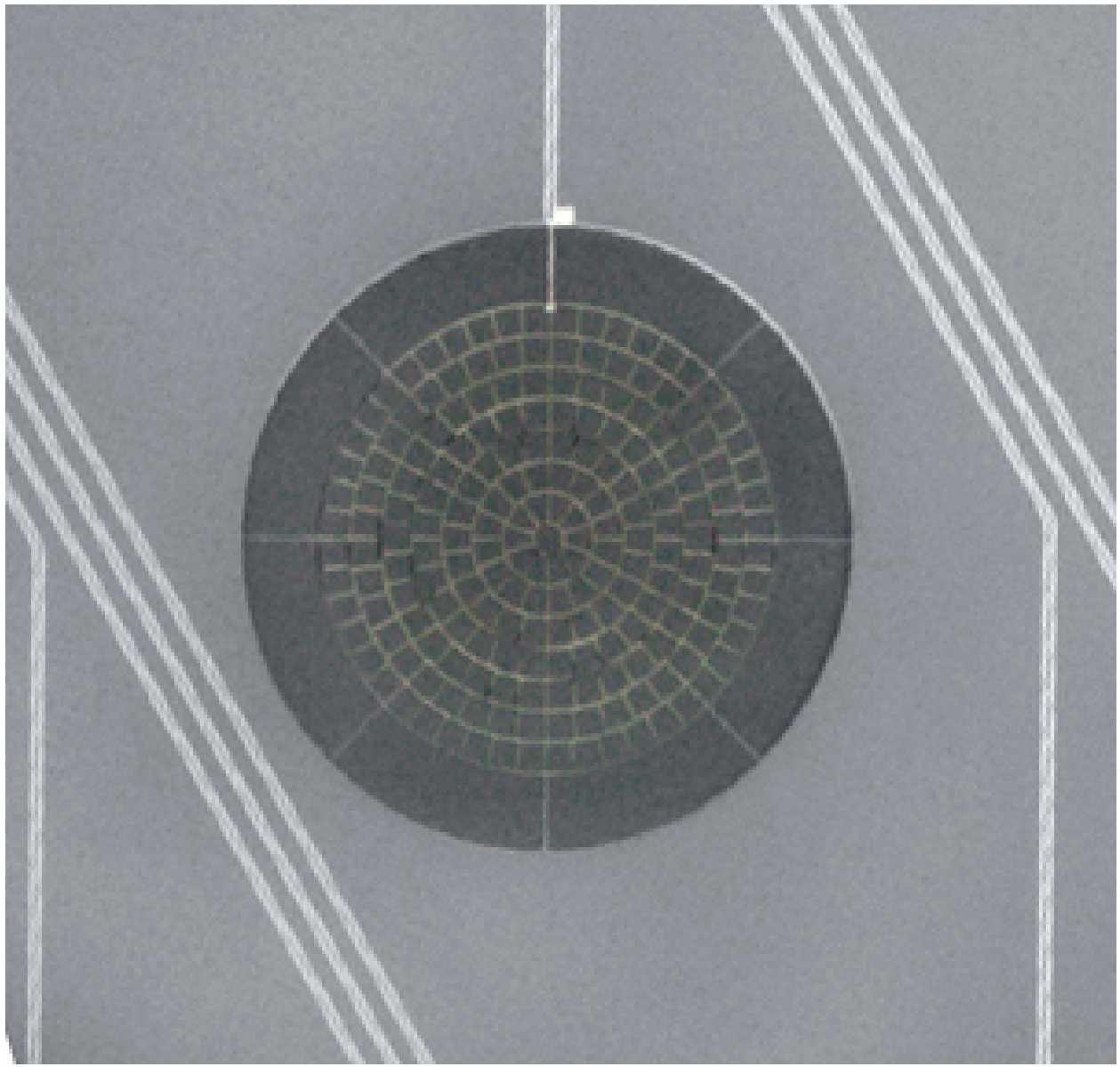

Focal Plane Design for APEX-SZ and SPT

Disk with machined conical horns positioned above bolometer arrray.

Horns match optics to bolometer plane.

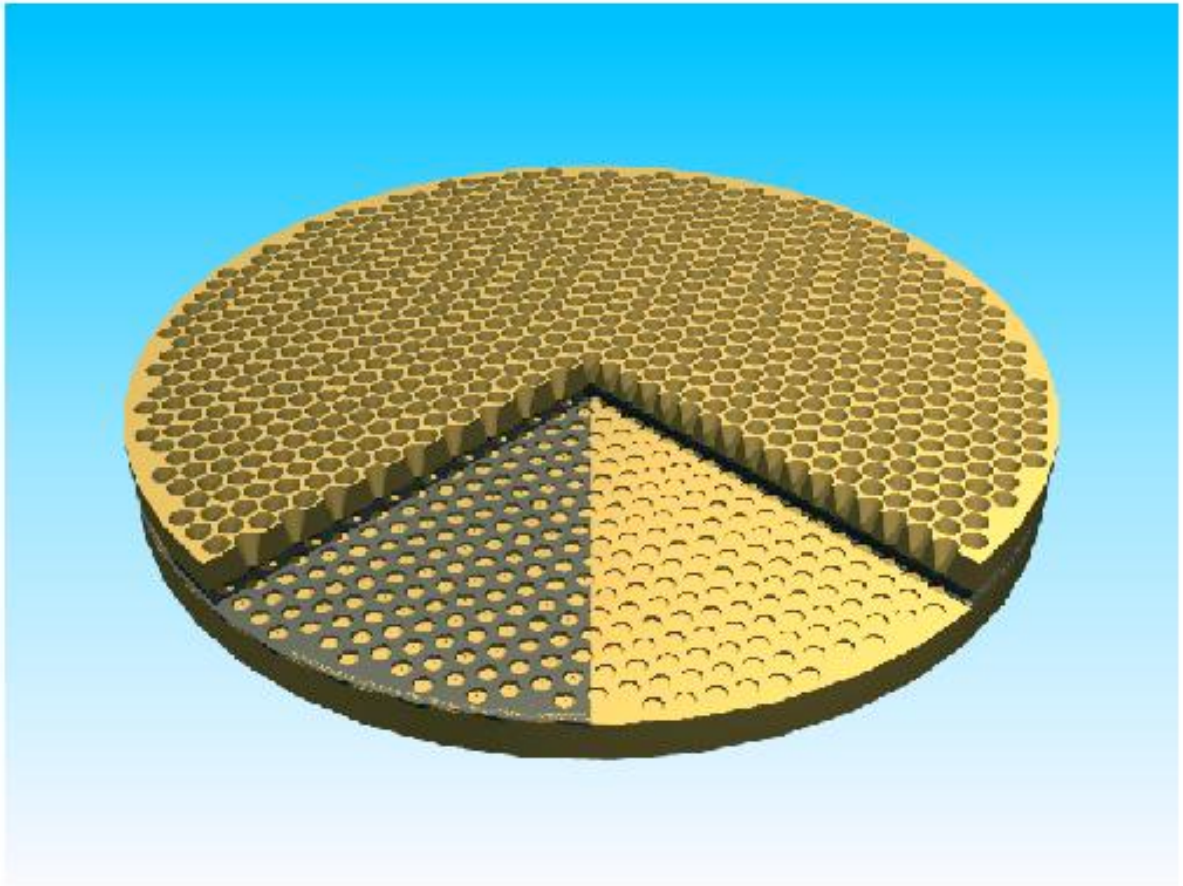

ANTENNA COUPLED BOLOMETERS

Antenna-Coupled Prototype Pixel (Mike Myers)

Microstrip Transmission Lines

Bandpass Filters (217 GHz, 40% BW)

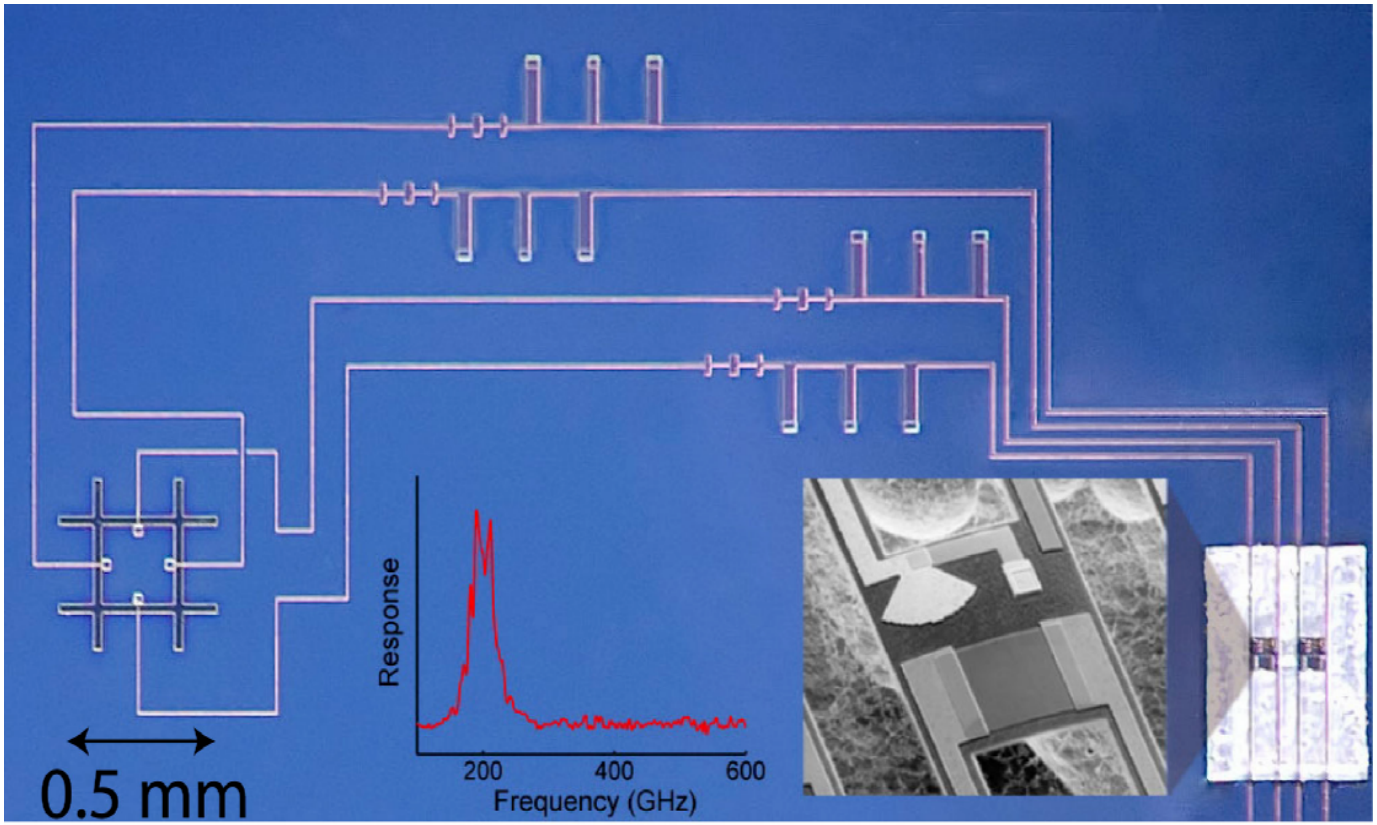

Microstrip terminated on a Si-nitride suspension.

Power measured with TES

Double-Slot Dipole Antenna

PolarBear Array Segment (Kam Arnold) – 90, 150, 220 GHz bands

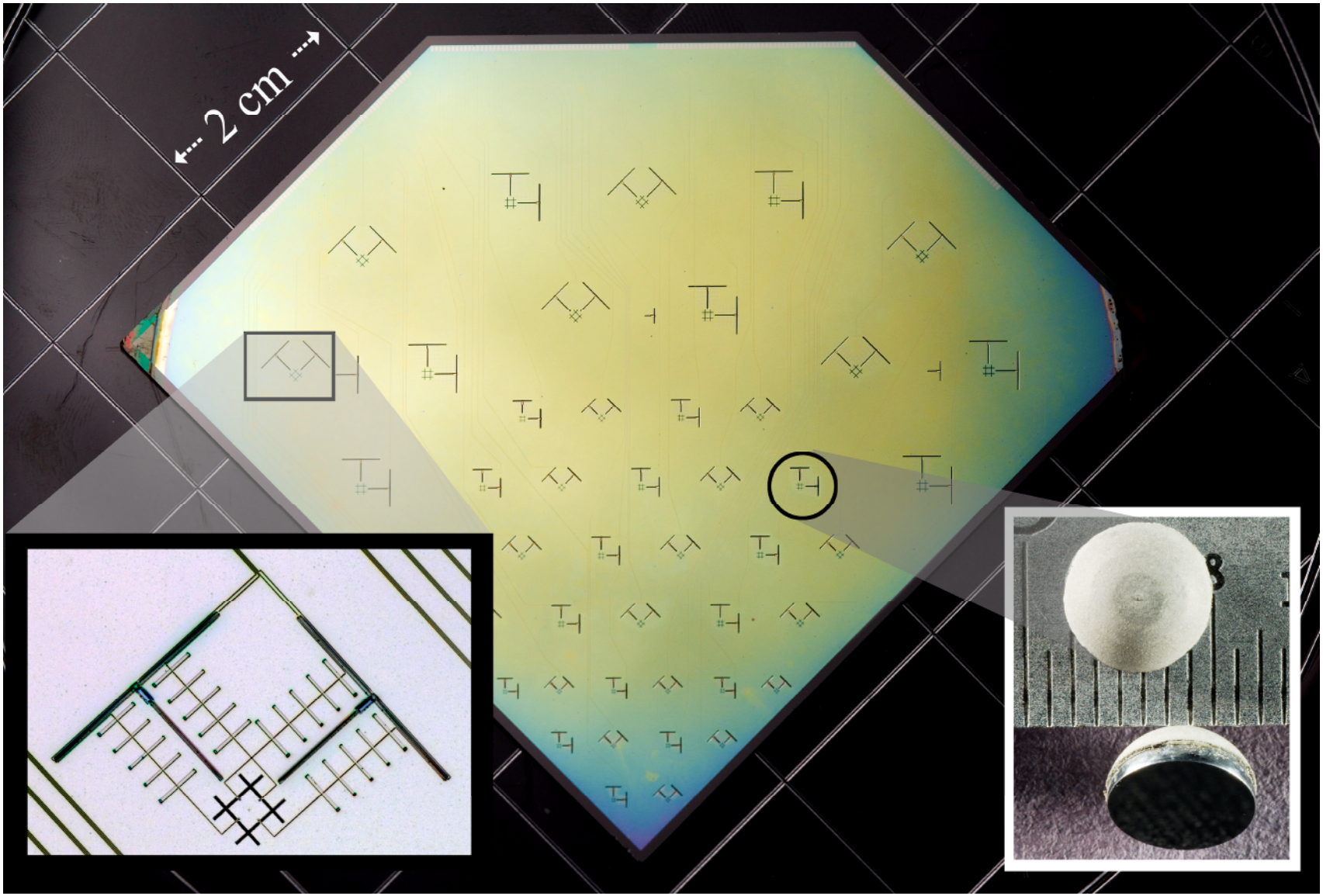

Antenna Coupling to Optics by Dielectric (Si) Lenses

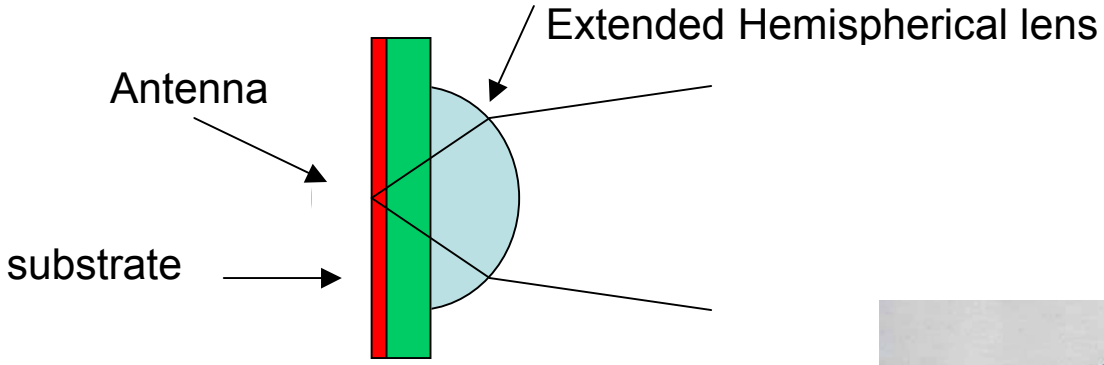

- Well developed (SIS mixers, etc.)
- High antenna gain, symmetric beam
- Forward radiation pattern
- Efficient coupling to telescope (similar to scalar horn)
- Complete pixel fits beneath lens
- Wideband AR coating (Erin Quealy)
- Broadband for multichroic pixels

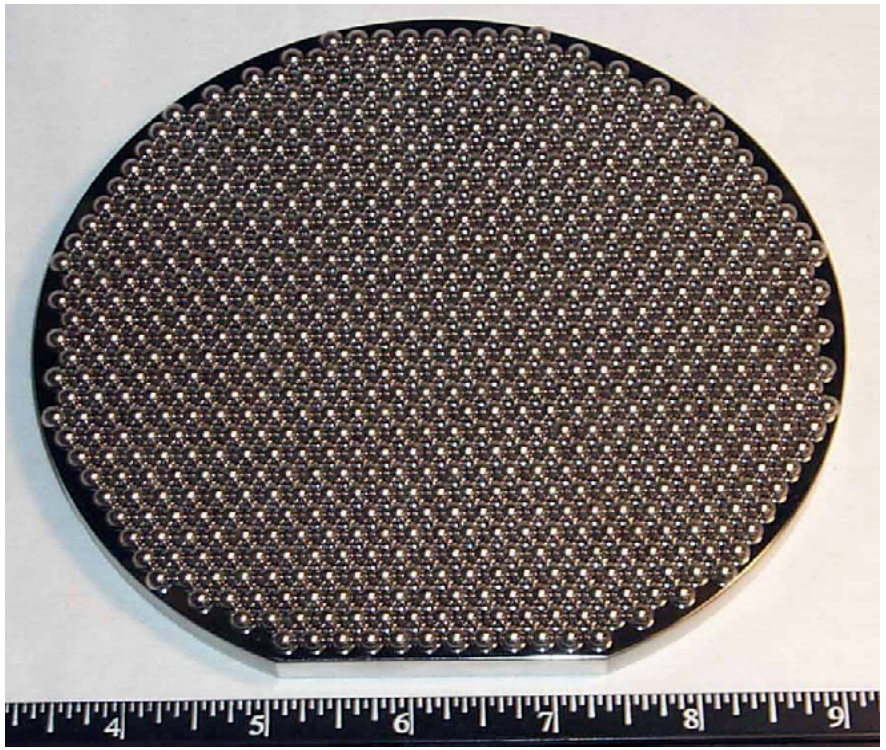

Future Development: Wideband Polarization-Sensitive Antenna + "Channelizer"

$\Rightarrow$ Multi-Frequency Pixel

GHz Scale Model:

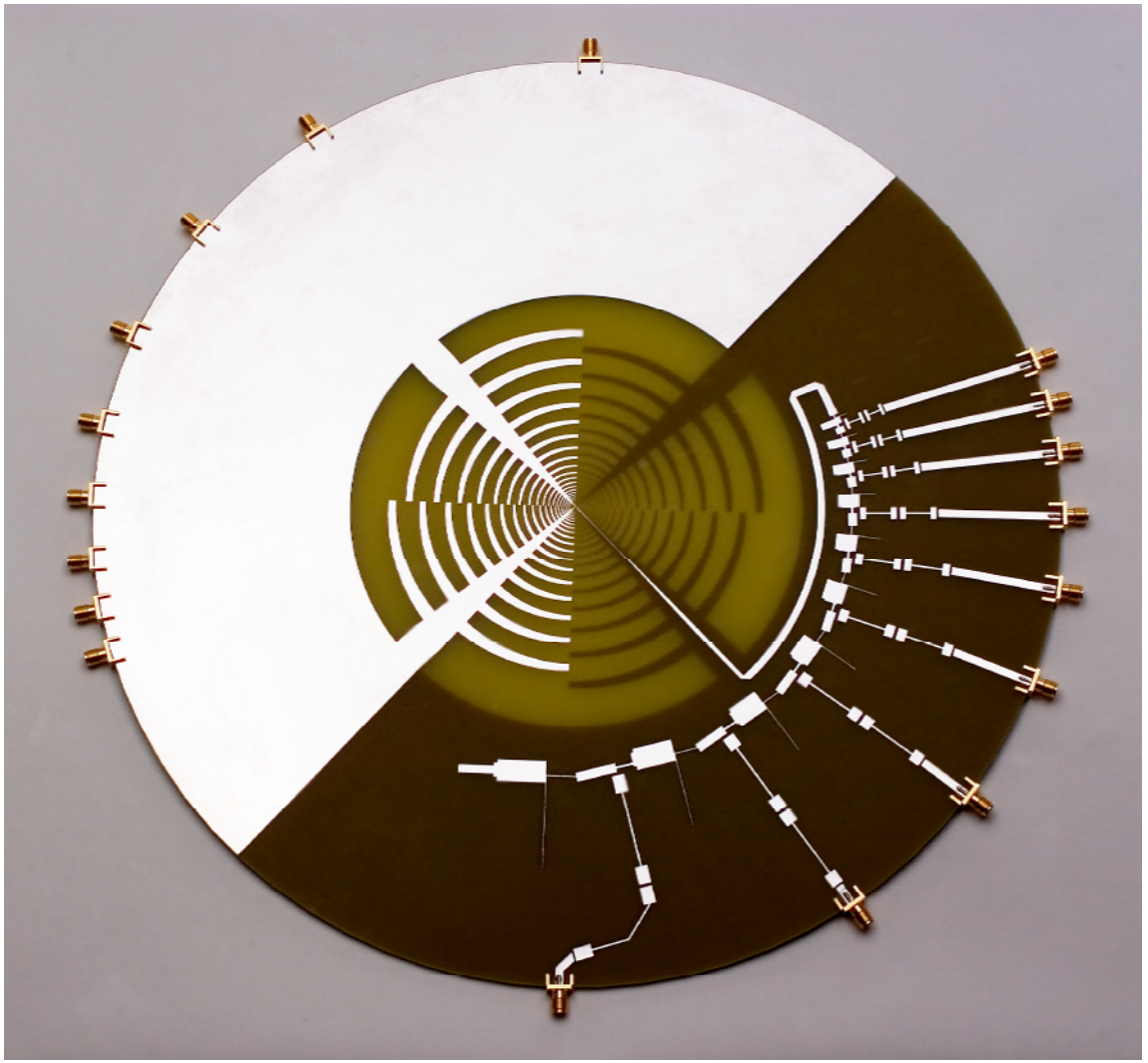

THz pixel with 3 bands currently in fab

(Roger O'Brient + Greg Engargiola)

READOUT

Readout

- Constant voltage bias requires that readout impedance $\ll$ bolometer resistance

  bolometer resistance $\approx 1\ \Omega$

  bias resistance $\approx 20\ \mathrm{m}\Omega$

  amplifier input impedance $\approx 10\ \mathrm{m}\Omega$

  1st amplifier stage: SQUID at 4K in shunt feedback configuration. High-frequency feedback loop includes SQUID + warm electronics (300K).

- Typical bolometer bias power: 10 – 40 pW

- Power Budget on 0.25K stage: <10 μW

- Heat conduction through wires to 4K stage acceptable up to ~300 bolometers

  $\Rightarrow$ Larger arrays require multiplexing

- Novel development:

  Frequency-Domain MUX with ZERO additional power on cold stage

Principle of Frequency-Domain Multiplexing

1. High-frequency bias (~100 kHz – 1 MHz)

   Each bolometer biased at different frequency

2. Signals change sensor resistance

   ⇒ Modulate current

   ⇒ Transfer signal spectrum to sidebands adjacent to bias frequency

   ⇒ Each sensor signal translated to unique frequency band

3. Combine all signals in common readout line

4. Retrieve individual signals in bank of frequency-selective demodulators

⇒ High-frequency bias provides greatly reduced sensitivity to microphonics

Modulation Basics

If a sinusoidal current $I_0 \sin \omega_0 t$ is amplitude modulated by a second sine wave $I_m \sin \omega_m t$

$$I(t) = (I_0 + I_m \sin \omega_m t) \sin \omega_0 t$$
$$I(t) = I_0 \sin \omega_0 t + I_m \sin \omega_m t \sin \omega_0 t$$

Using the trigonometric identity $2 \sin \alpha \sin \beta = \cos(\alpha - \beta) - \cos(\alpha + \beta)$ this can be rewritten

$$I(t) = I_0 \sin \omega_0 t + \frac{I_m}{2} \cos(\omega_0 t - \omega_m t) - \frac{I_m}{2} \cos(\omega_0 t + \omega_m t)$$

The modulation frequency is translated into two sideband frequencies

$(\omega_0 t + \omega_m t)$ and $(\omega_0 t - \omega_m t)$

symmetrically positioned above and below the carrier frequency ω_0.

All of the information contained in the modulation signal appears in the sidebands; the carrier does not carry any information whatsoever.

The power contained in the sidebands is equal to the modulation power, distributed equally between both sidebands.

Modulation Waveforms and Spectra

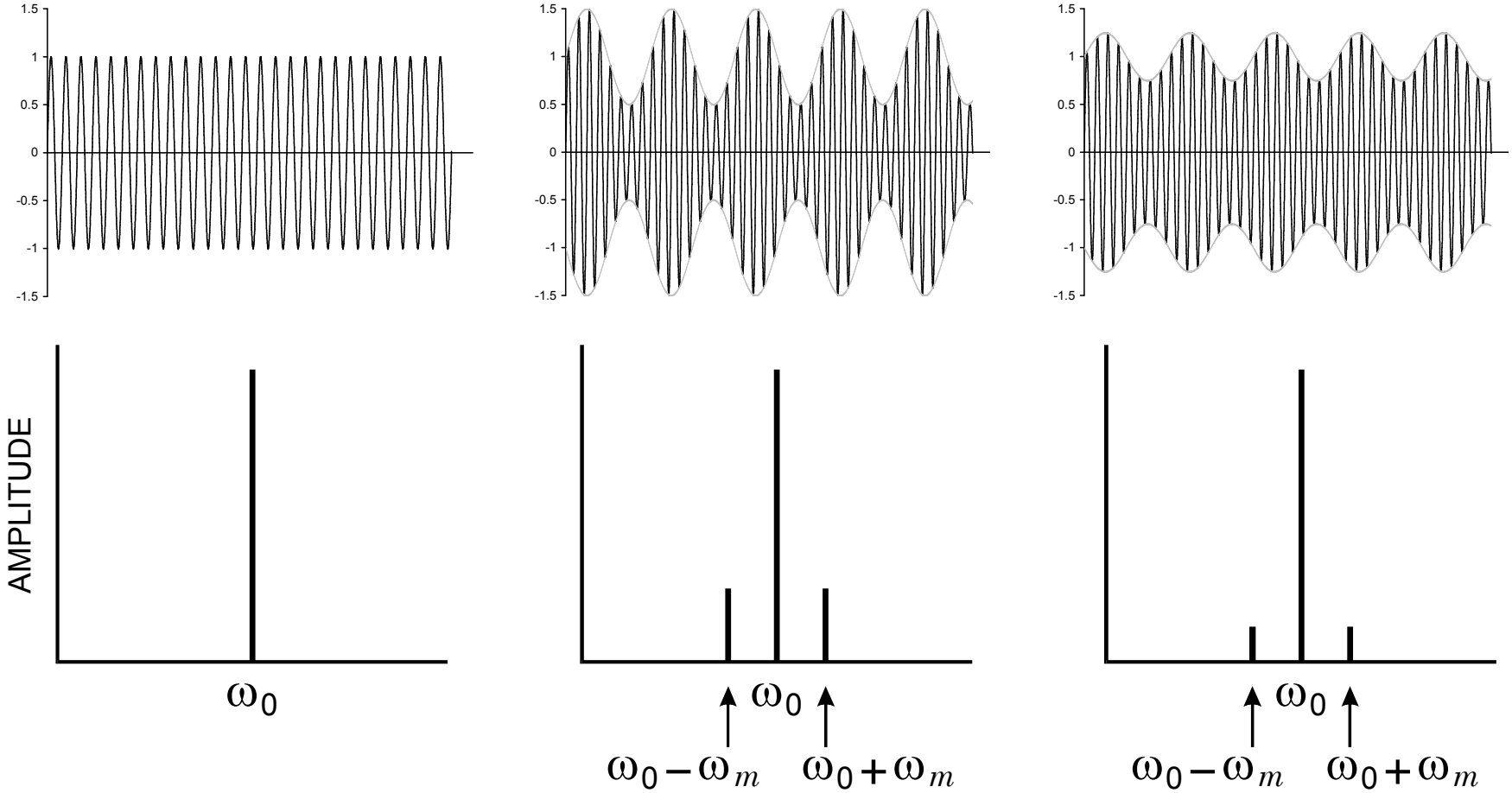

Carrier amplitude remains constant! All signal information in the sidebands.

MUX circuit on cold stage

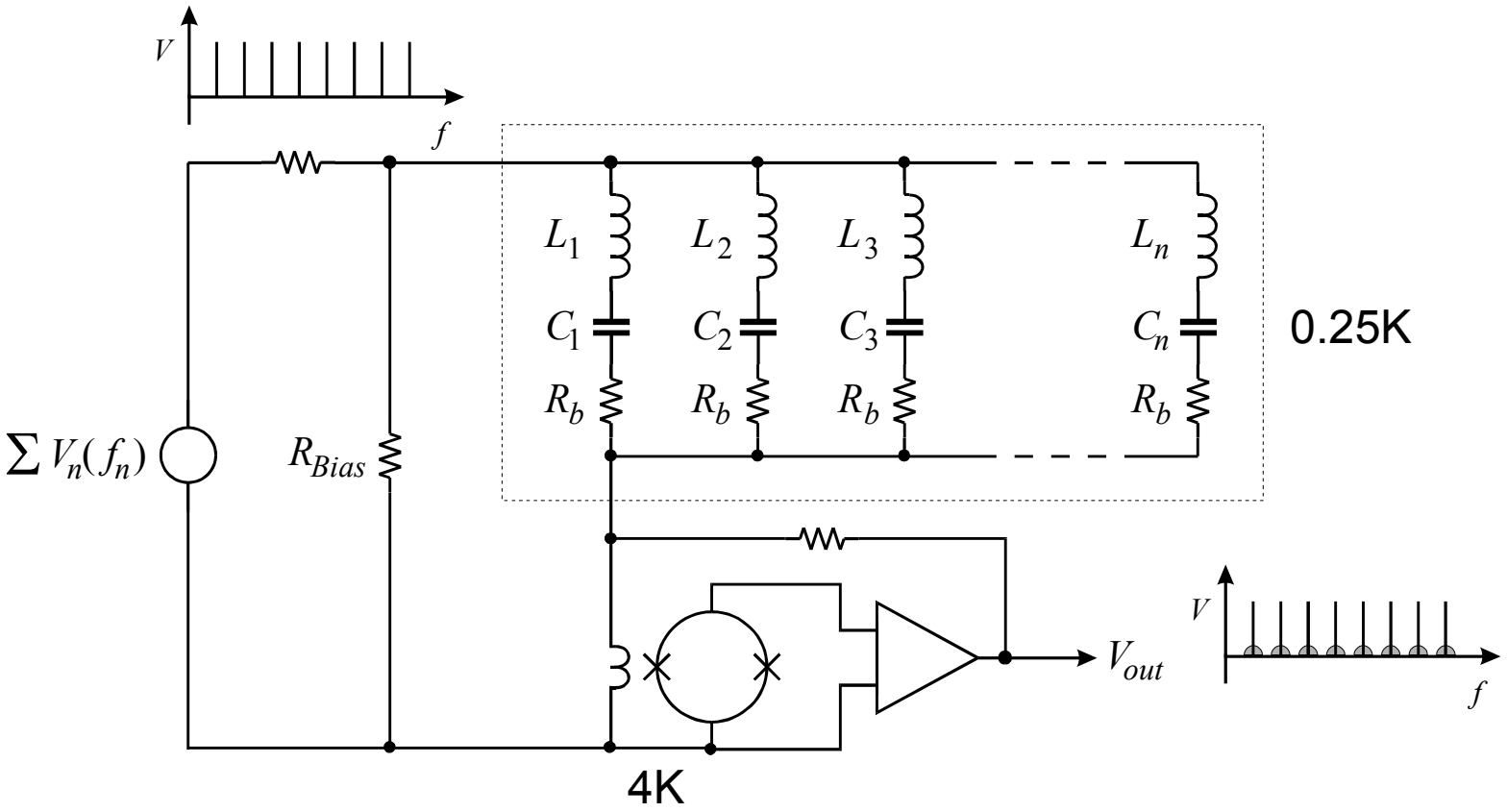

- "Comb" of all bias frequencies fed through single wire.
- Tuned circuits "steer" appropriate frequencies to bolometers and limit noise bandwidth.
- Wiring inductance tuned out at resonance to reduce impedance.
- Current return through shunt-fedback SQUID amplifier (low input impedance).
- No additional power dissipation on cold stage (only bolometer bias power).

Constraints on Tuned Circuits

Selectivity and spacing of tuned circuits determines cross-talk.

However:

Limited bandwidth introduces additional time constant into electro-thermal negative feedback.

Analogous to multiple cutoff frequencies ("poles") in electronic feedback systems.

If bandwidth too small, bias power cannot respond quickly enough to changes in optical power

⇒ Instability!

⇒ Bolometer time constants must be compatible with MUX parameters.

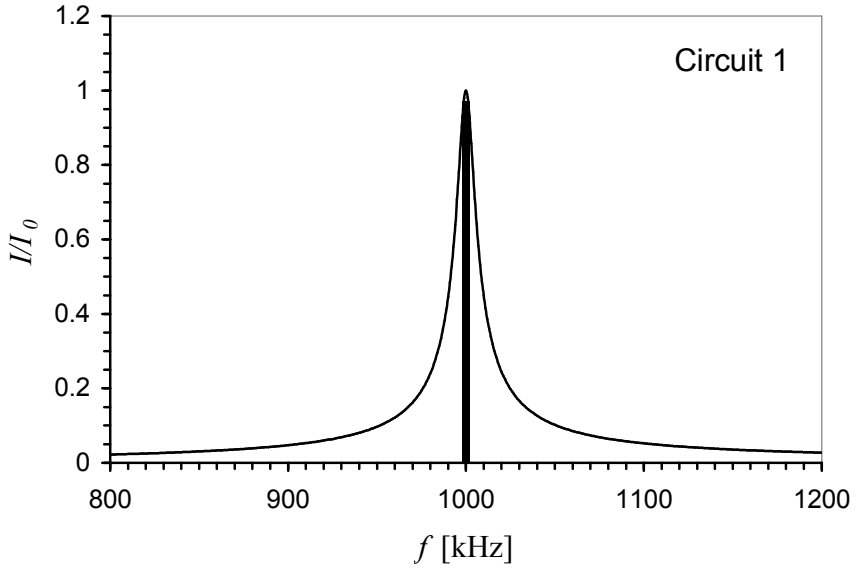

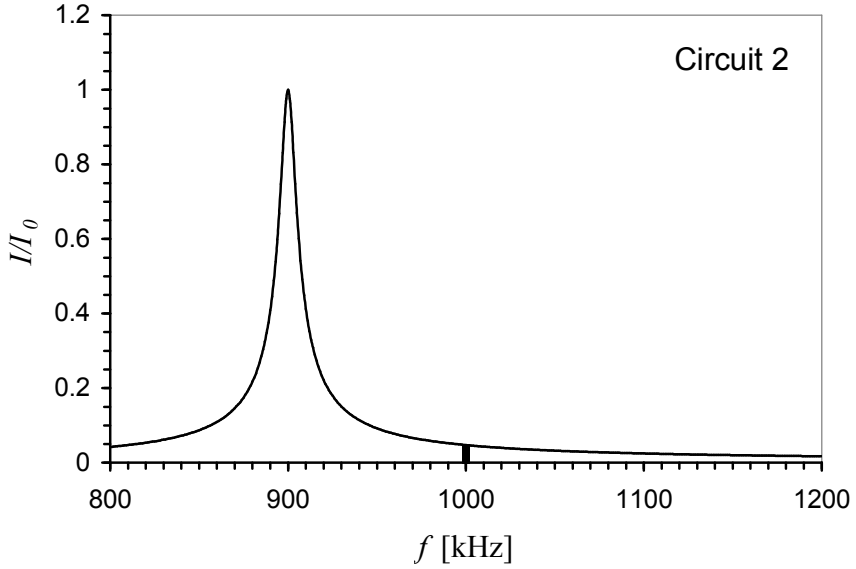

Demodulation

The same carrier signal that biases the sensor is used to translate the sideband information to baseband.

The mixer acts analogously to a modulator, where the input signal modulates the carrier, forming both sum and difference frequencies.

In the difference spectrum the sidebands at $f_n \pm \Delta f_S$ are translated to a frequency band

$$f_n - (f_n \pm \Delta f_S) = 0 \pm \Delta f_S .$$

A post-detection low-pass filter attenuates all higher frequencies and determines the ultimate signal and noise bandwidth.

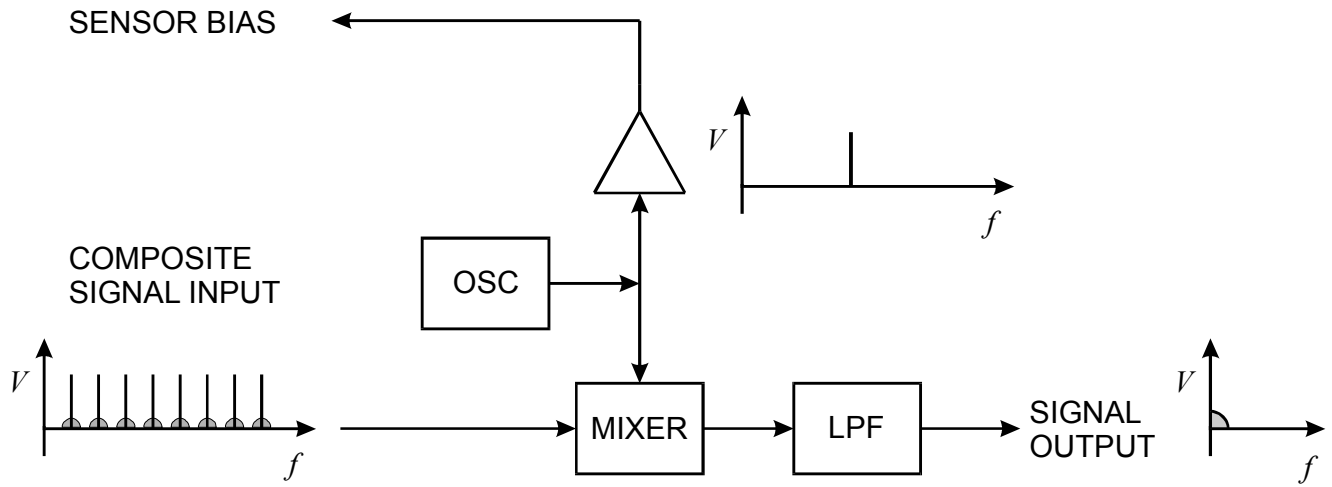

- We use a highly linear sampling demodulator that aliases the high-frequency signal to baseband.

SQUIDs

Superconducting Quantum Interference Devices

Two Josephson junctions connected in parallel to form superconducting ring:

Two key ingredients:

1. Phase between two tunneling currents in Josephson junction is determined by current.

2. Magnetic flux in superconducting loop is quantized:

$$\Delta\Phi_0 = \frac{\pi\hbar c}{e} = 2.0678 \cdot 10^{-7} \text{ gauss cm}^2$$
$$= 2.0678 \cdot 10^{-15} \text{ Vs}$$

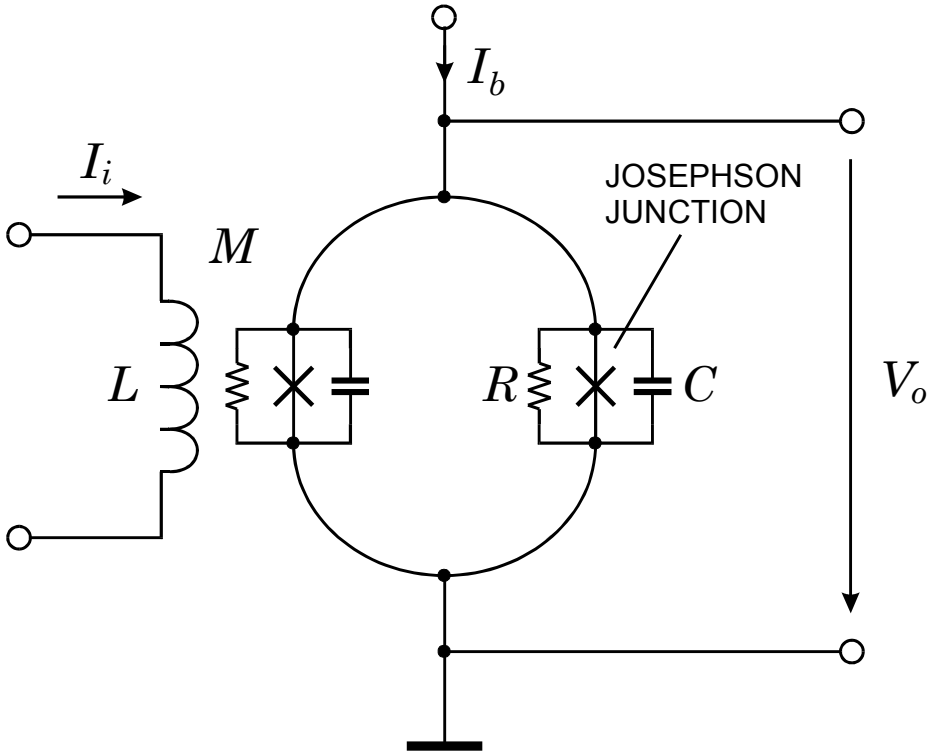

SQUID is biased by current I_b.

- Input signal is magnetic flux due to current through coupling coil L.
- Output is voltage V_o .

Current-Voltage Characteristics:

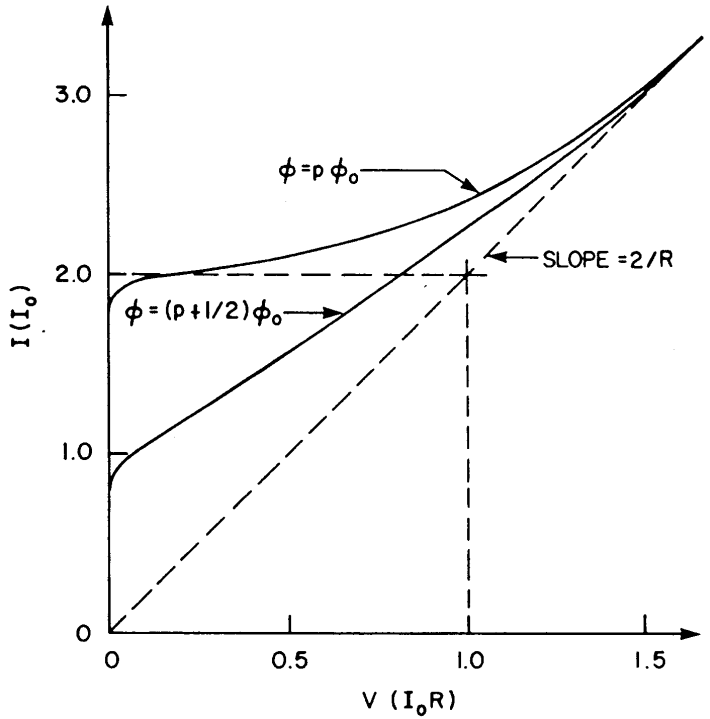

Output voltage V vs. flux Φ/Φ_0 as bias current I_B is increased

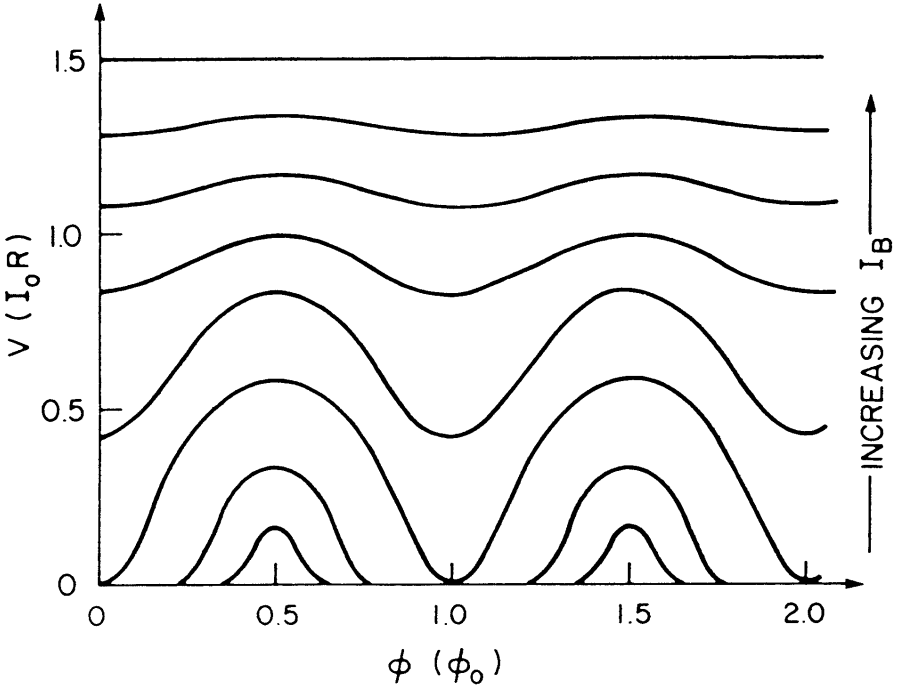

However,

- Input signal may not exceed ¼ flux quantum (output periodic in Φ_0)
- Feedback loop required to lock flux at proper operating point (flux locked loop)

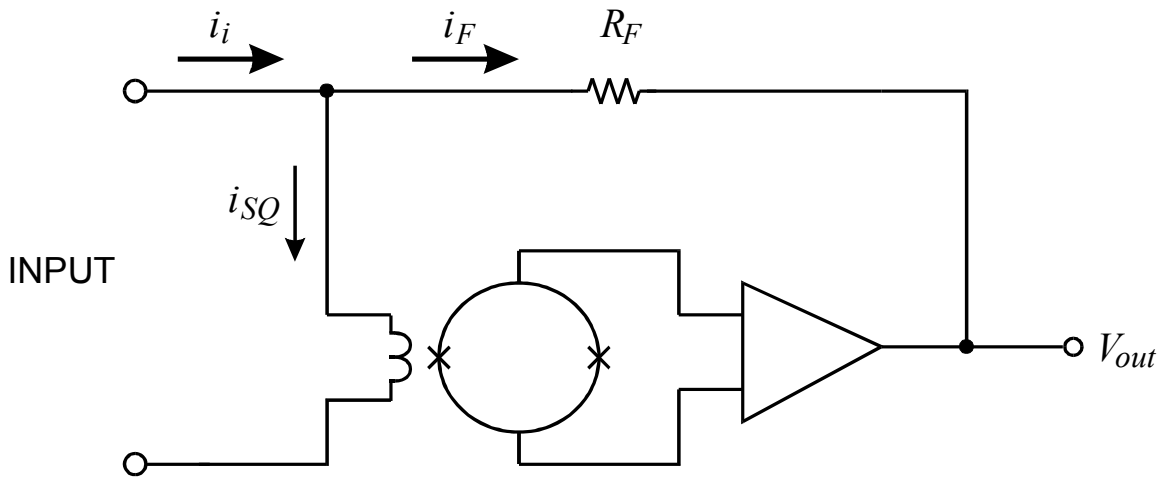

Maximum acceptable signal level grows with increasing loop gain.

Voltage bias requires input impedance ≪ bolometer resistance!

Shunt feedback SQUID amplifier achieves about 10 mΩ at 1 MHz

However: Feedback circuit limits frequency response.

Typical Parameters

Operating Temperature:	0 – 5 K (also for high T_C SQUIDs: noise)
Flux Sensitivity:	V_Φ =150 μV/Φ_0
Flux Noise:	1 to 10 μΦ_0
SQUID Inductance:	100 – 500 pH
Input Inductance:	10 nH to 1 μH

Series SQUID Arrays

Array of SQUIDs with
input coils in series and
outputs connected in series.

We use arrays of 100 series-connected SQUIDs (fabricated by NIST).

Sensitivity : $\dfrac{\text{output voltage}}{\text{input current}} = M_i \dfrac{dV}{d\Phi} \approx 500$

Bandwidth Limit of Feedback Loop

At low frequencies phase shift = 180° (negative feedback)

All systems incur additional phase shift

amplifier (additional time constants at high frequencies)

propagation delay of wiring

parasitic resonances

Criterion for stability against self-oscillation:

At frequency where total phase shift in feedback loop is 360°,

gain of feedback loop (loop gain) <1

Commonly used criterion to minimize ringing: phase margin = 45°

i.e. additional phase shift 135°

Phase shift vs. frequency from wiring (wire length 1 m round trip)

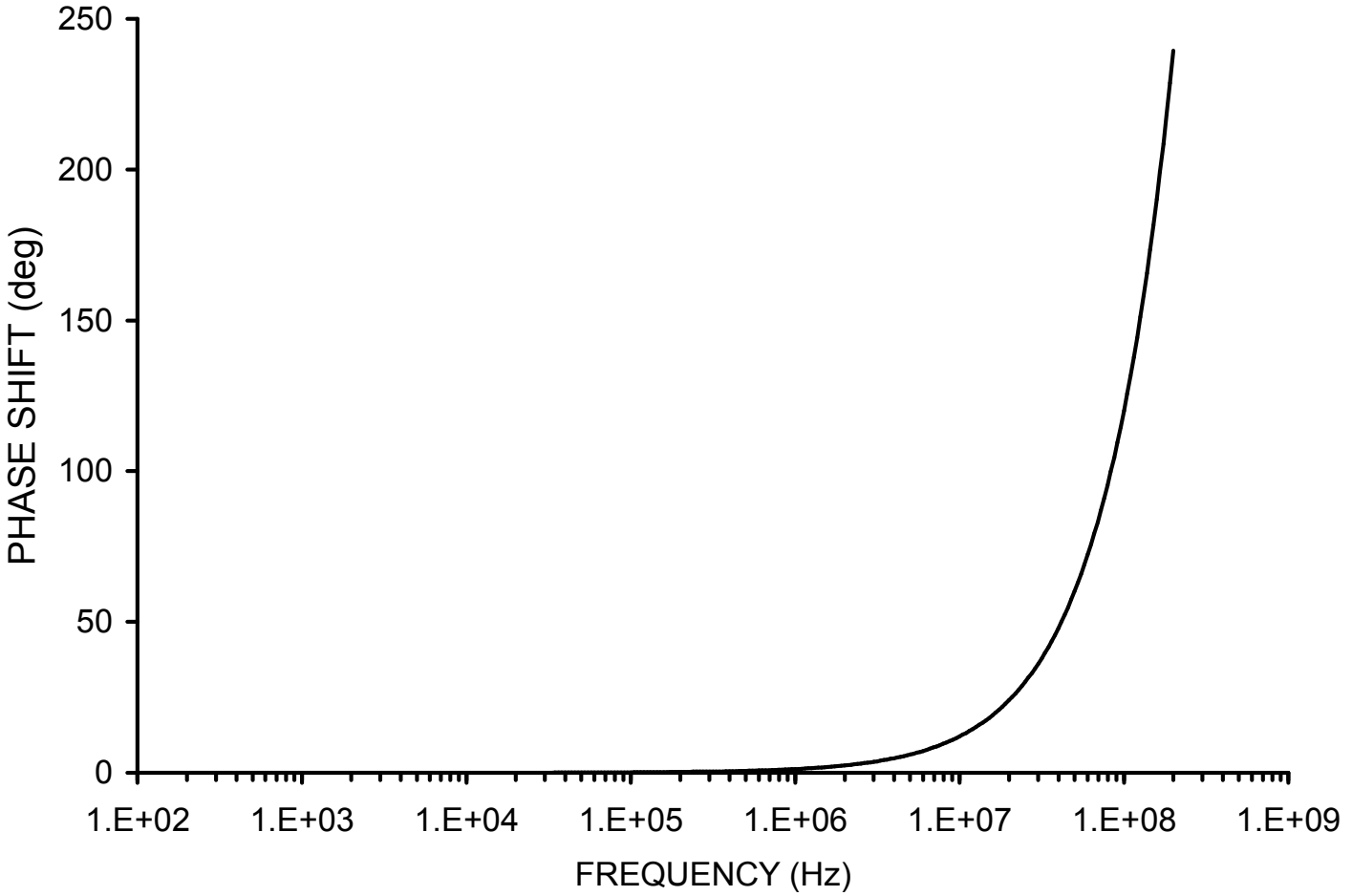

If feedback loop gain is >1 at the frequency where the phase shift is 180°, the system will oscillate

⇒ must limit frequency response!

Additional phase shift vs. frequency from wiring + amplifier

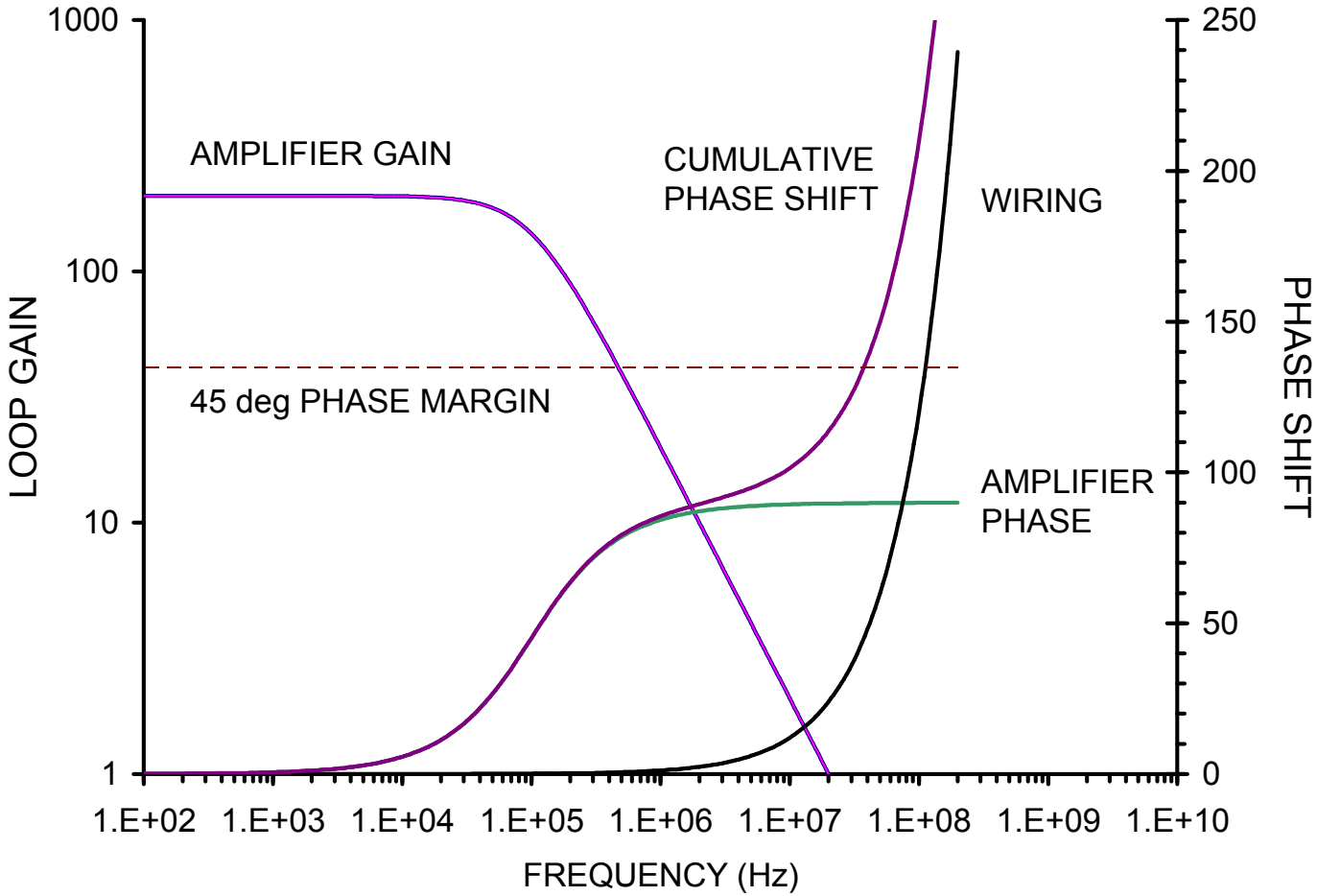

Examples:

SQUID's allowable input signal increased by loop gain.

Example: input signal of $25\Phi_0$ requires loop gain $A_L \approx \frac{25\Phi_0}{\Phi_0/4} = 100$

Stable operation requires that loop gain roll off to unity at frequency where net phase shift is at least 45° (phase margin).

⇒ relative to 180° phase shift at low frequencies, can tolerate additional 135° phase shift.

Single pole response introduces 90° phase shift beyond cutoff frequency f_{max}

⇒ connecting leads are allowed to introduce additional 45° phase shift.

Lead length l with phase velocity v_p ⇒ $\Delta\varphi = \frac{lf}{v_P} 2\pi$

⇒ unity gain frequency $f_0 = \frac{v_P}{8l}$

⇒ loop gain-bandwidth product $A_L f_{\max} = \frac{v_P}{8l}$

⇒ cutoff frequency $f_{\max} = \frac{v_P}{8lA_L}$

a) bare wire

$$v_P = c$$

$$l = 30\ \text{cm} \quad \Rightarrow \quad A_L f_{max} = 125\ \text{MHz}$$ (loop gain-bandwidth product)

$$A_L = 100 \quad \Rightarrow \quad f_{max} = 1.25\ \text{MHz}$$

b) coaxial cable or twisted pair

$$v_P = \frac{c}{\sqrt{\varepsilon}} = \frac{2}{3}c$$

$$l = 30\ \text{cm} \quad \Rightarrow \quad A_L f_{max} \approx 80\ \text{MHz}$$

$$A_L = 100 \quad \Rightarrow \quad f_{max} \approx 0.8\ \text{MHz}$$

$\Rightarrow$ Low frequency operation (~ 1 MHz) requires controlled phase at high frequencies (~100 MHz)

$\Rightarrow$ minimize physical length of feedback loop!

localized cold loop advantageous

$\Rightarrow$ Limits to achievable feedback loop gain, so additional technique employed.

Feedback crucial to linearize SQUID response: Intermodulation

SQUID output voltage approx. sinusoidal function of flux

$$\Rightarrow \quad \text{non-linear:} \qquad \sin x \approx x - \frac{x^3}{3!} + \frac{x^5}{5!} \ \ldots$$

Non-linear terms lead to mixing products:

$$(\sin \omega_1 t + \sin \omega_2 t)^n = \left((e^{\mathbf{i}\omega_1 t} - \mathbf{i}e^{-\mathbf{i}\omega_1 t}) + (e^{\mathbf{i}\omega_2 t} - \mathbf{i}e^{-\mathbf{i}\omega_2 t}) \right)^n$$

For two input frequencies f_1 and f_2: 3^{rd} order distortion $\Rightarrow$

- $3 f_1$
- $3 f_2$
- $2 f_1 \pm f_2$
- $2 f_2 \pm f_1$

What levels are of concern?

Bolometer noise current:	10 pA/Hz$^{1/2}$
Bandwidth:	100 Hz
Total noise current:	100 pA
Bolometer bias current:	10 μA
i_{noise} / i_{bias} =	10^{-5} (-100 dBc)

System must be designed for very low distortion – choose appropriate technology

Carrier Nulling

Maximum input signal to SQUID is limited, even with feedback (“flux jumping”)

All of the information is in the sidebands, so the carrier can be suppressed to reduce dynamic range requirements.

Low-frequency sideband noise associated with carriers cancels (-110 dBc at 10 Hz)

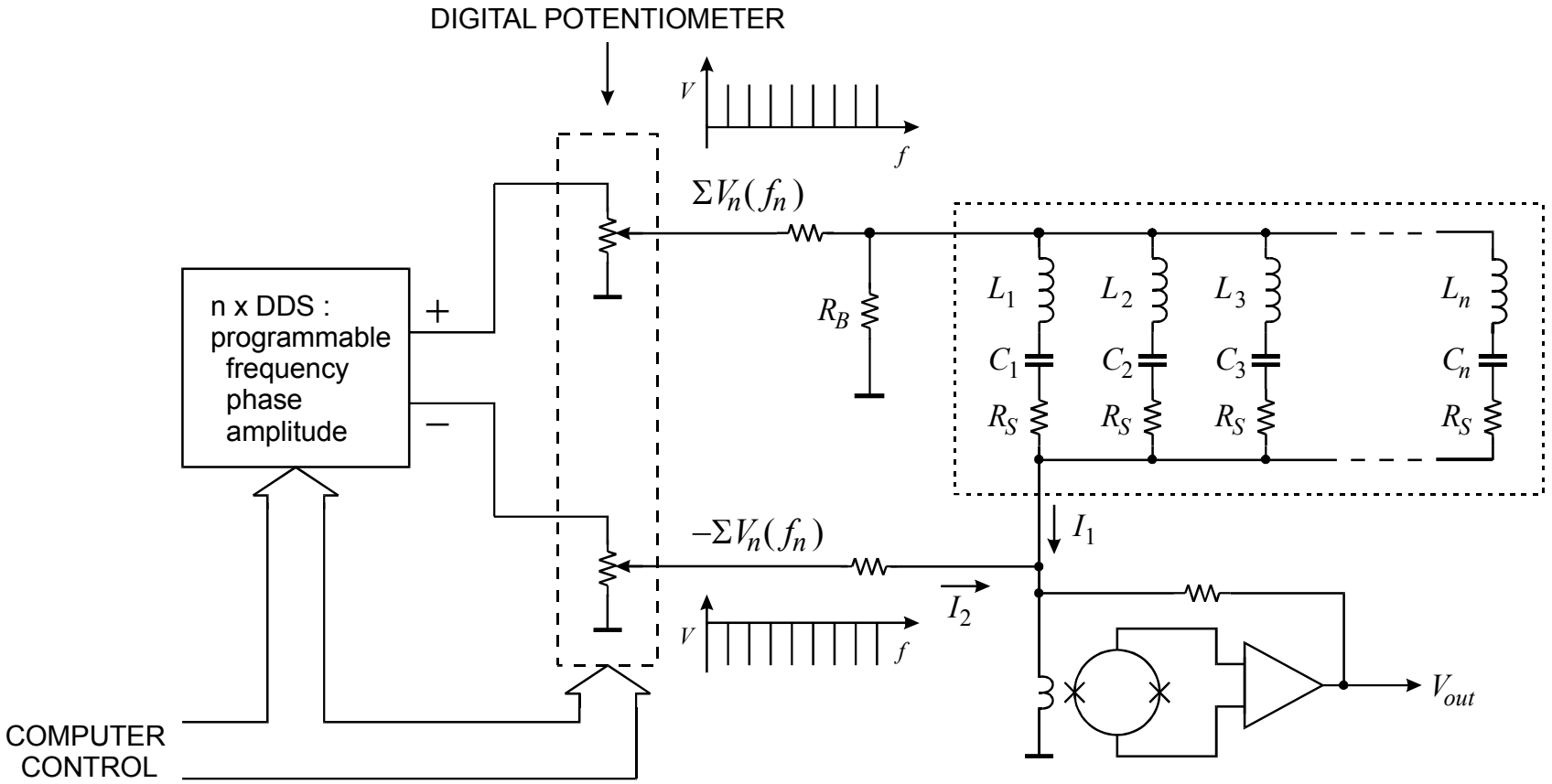

Sideband Noise

All frequency generators exhibit noise sidebands above and below the desired frequency.

Sideband noise of a high-quality frequency synthesizer:

At frequencies <10 Hz the noise is too large for our application.

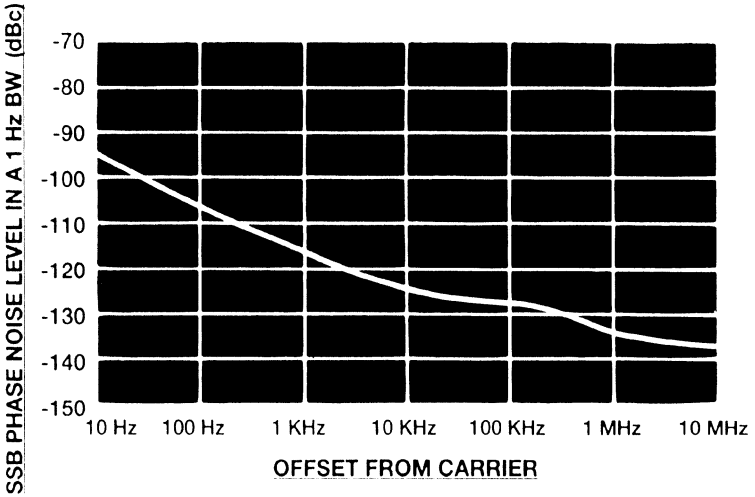

Very high-quality synthesizer:

We achieve similar results with direct digital synthesis (DDS).

Adequate for some observations, but we require somewhat lower noise levels, so the cumulative noise from independent carrier generators for bolometer biasing and nulling is too large.

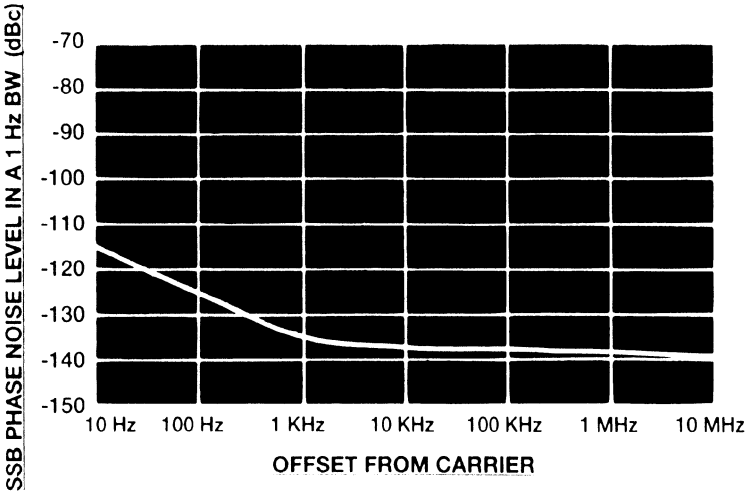

Demodulator

Frequency mixers are commonly described in terms of square law devices:

$$(\sin\omega_1 t + \sin\omega_2 t)^2 = \left((e^{\mathbf{i}\omega_1 t} - \mathbf{i}e^{-\mathbf{i}\omega_1 t}) + (e^{\mathbf{i}\omega_2 t} - \mathbf{i}e^{-\mathbf{i}\omega_2 t})\right)^2$$

yields terms $\omega_1 \pm \omega_2$, so a frequency spectrum $\omega_1 + \Delta\omega$ when mixed with a local oscillator ω_1 yields an output extending from zero to $\Delta\omega$.

However, there are no perfect square law devices, so additional mixing products are generated.

In the presence of many carriers high order intermodulation products will contaminate the signal bands.

Need a highly linear demodulator.

Sampling Demodulator

The signal spectrum $\omega_1 + \Delta\omega$ is sampled at the carrier frequency ω_1 :

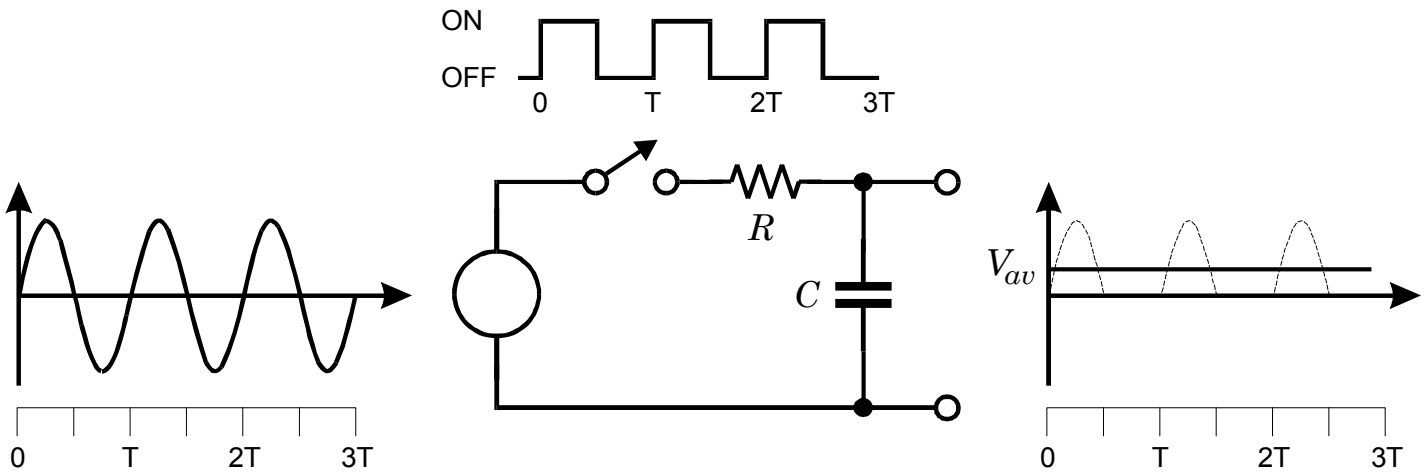

RESPONSE TO LOW-FREQUENCY MODULATION

No inherently non-linear devices needed. (old principle: synchronous rectifier)

Aliasing

When a signal is sampled at a frequency that is lower than the signal frequency it is “aliased” to lower frequencies:

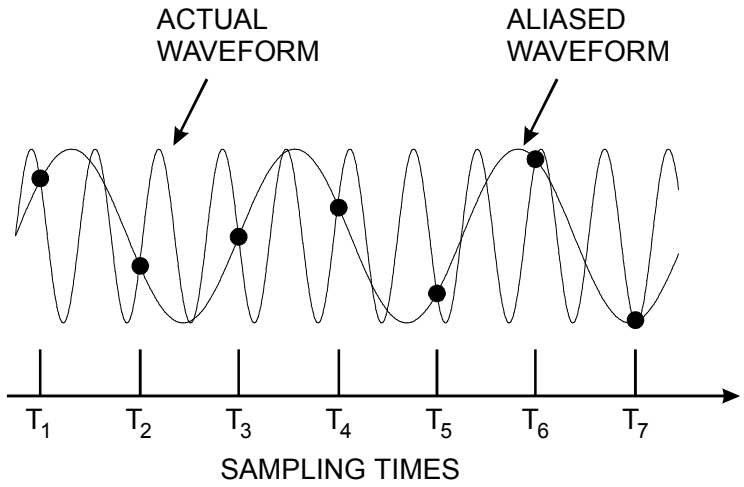

An input signal f_i sampled at a rate f_s yields signal components $f_i \pm k f_s$.

Applies to any form of sampling (time waveform, image, ...)

Nyquist condition: Sampling frequency > 2x highest signal frequency

We turn aliasing into a virtue:

Sampling at the carrier frequency aliases the signal spectrum to baseband.

We use a full-wave sampling demodulator for common-mode rejection

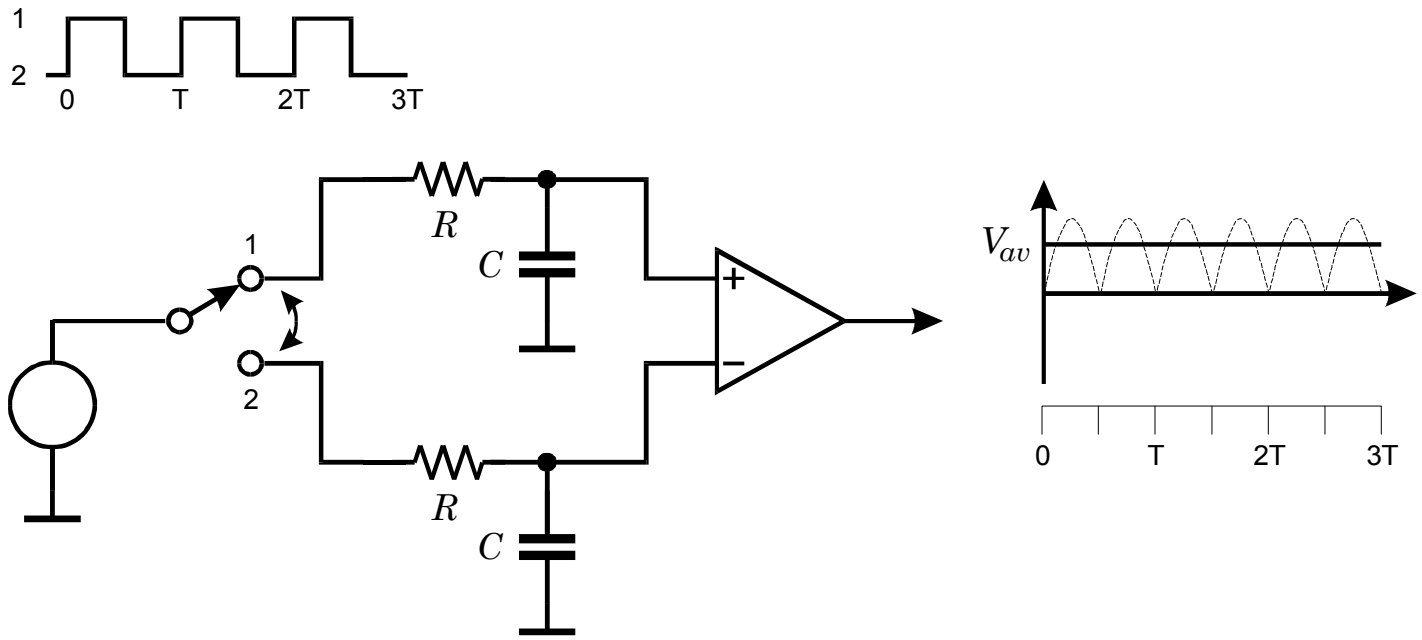

MOSFET switches used for commutation.

System Block Diagram

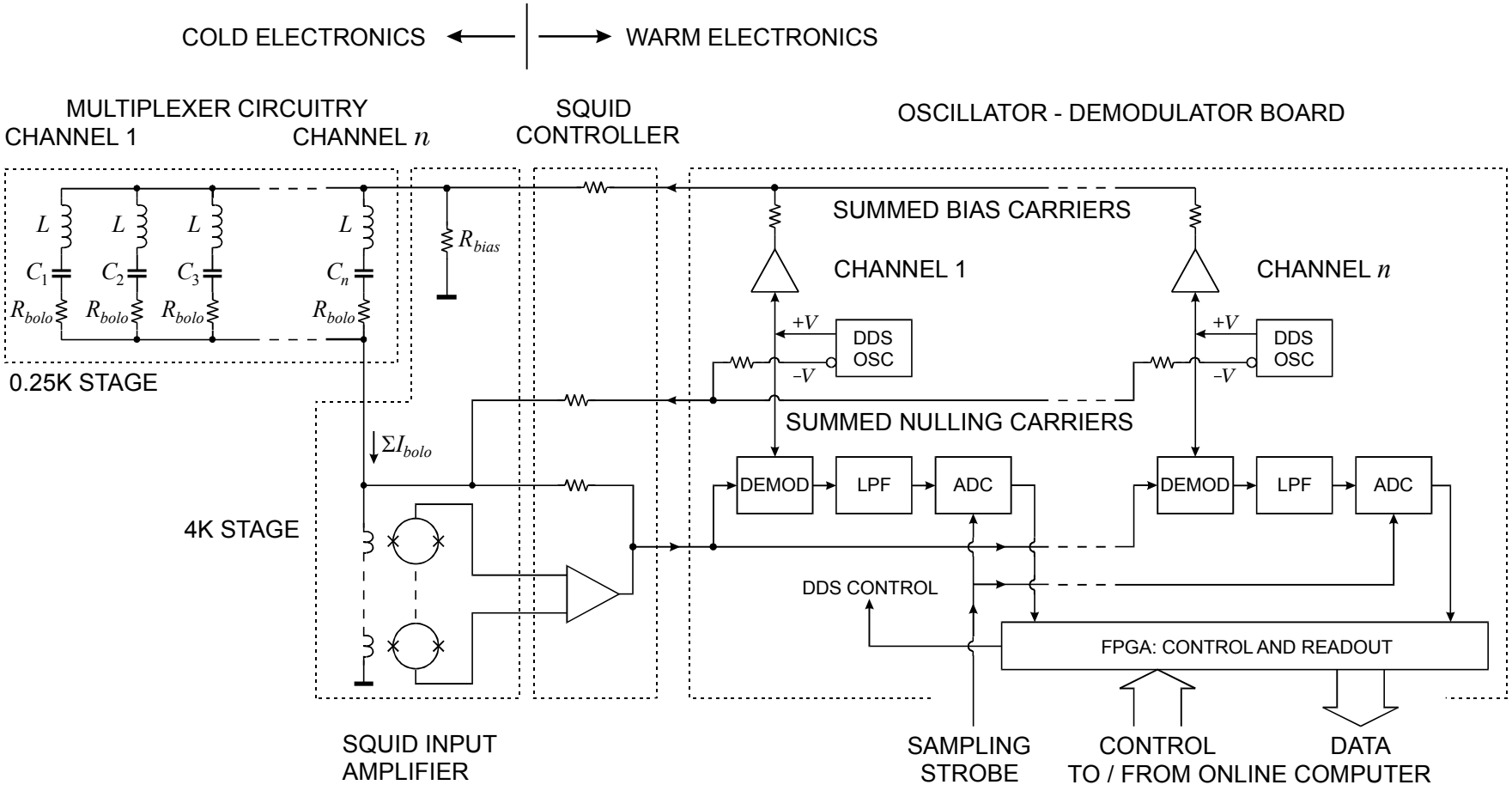

MUX chip (0.25K stage)

Superconducting spiral inductors integrated on a chip

(fabbed by Northrup-Grumman)

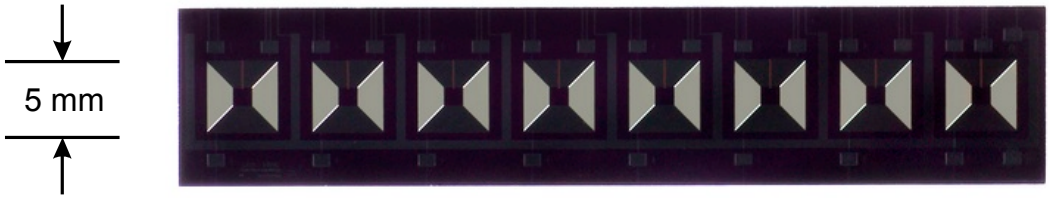

Capacitors can be integrated with inductors, but external chip capacitors require less space.

NP0 capacitors perform well at 4K

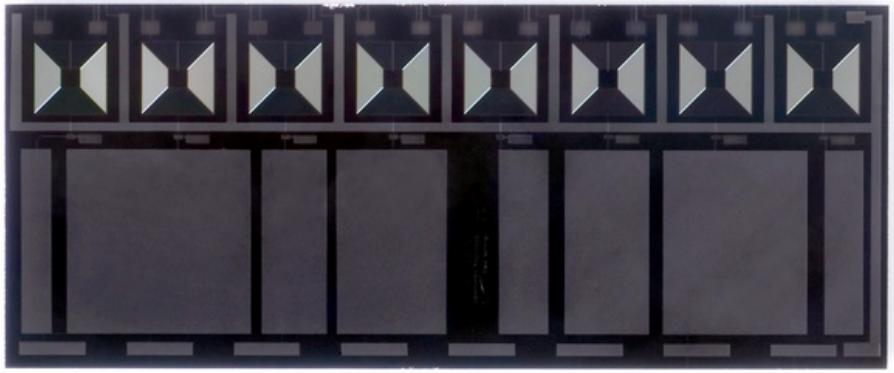

SQUIDs mounted as arrays of eight in magnetic shield (4K stage)

SQUID mounting board

SQUIDs mounted on Nb pads
to pin magnetic flux

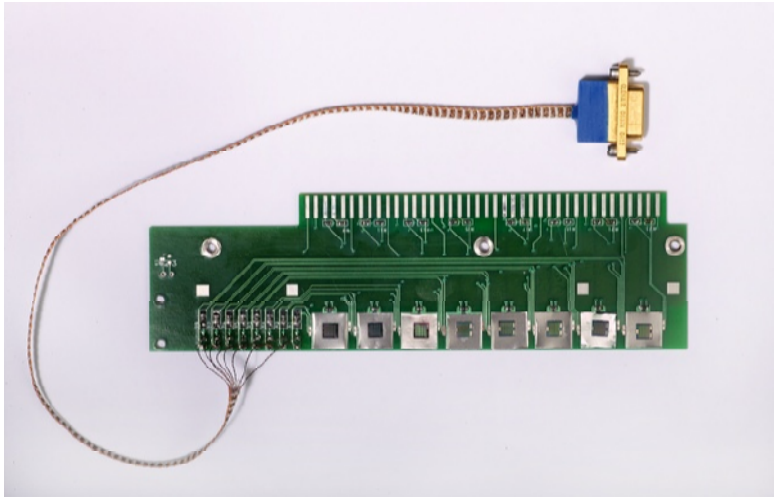

Magnetic Shield
(M. Lueker)

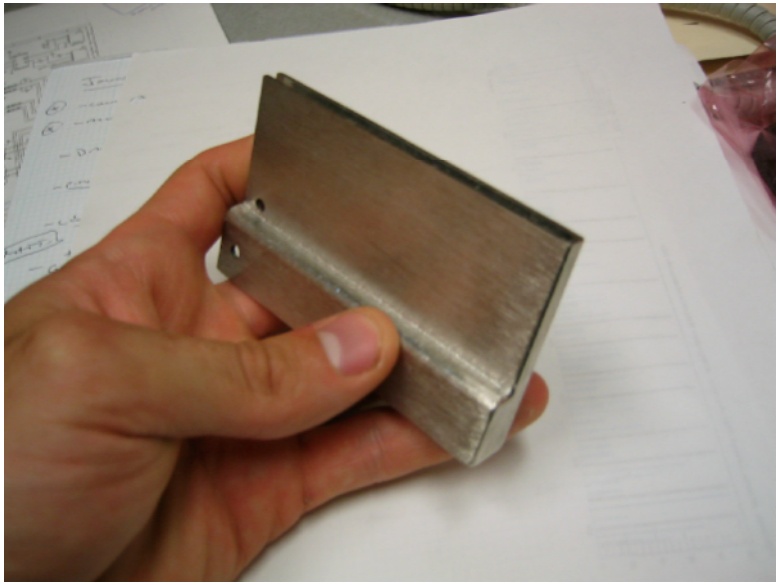

8-channel SQUID Controller

Computer-controlled (FPGA)
SQUID diagnostics
Open/closed loop
Switchable gain

SQUIDs VERY sensitive to pickup (up to GHz), so local shielding of digital circuitry is crucial.

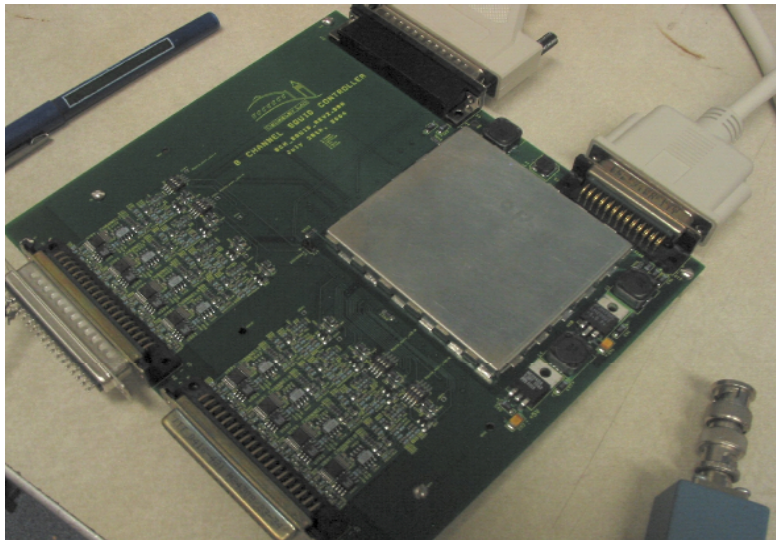

16-channel Demodulator Board

16 individual demodulator channels
1 DDS freq. generator per channel
On-board A/D
Opto-isolated computer interface

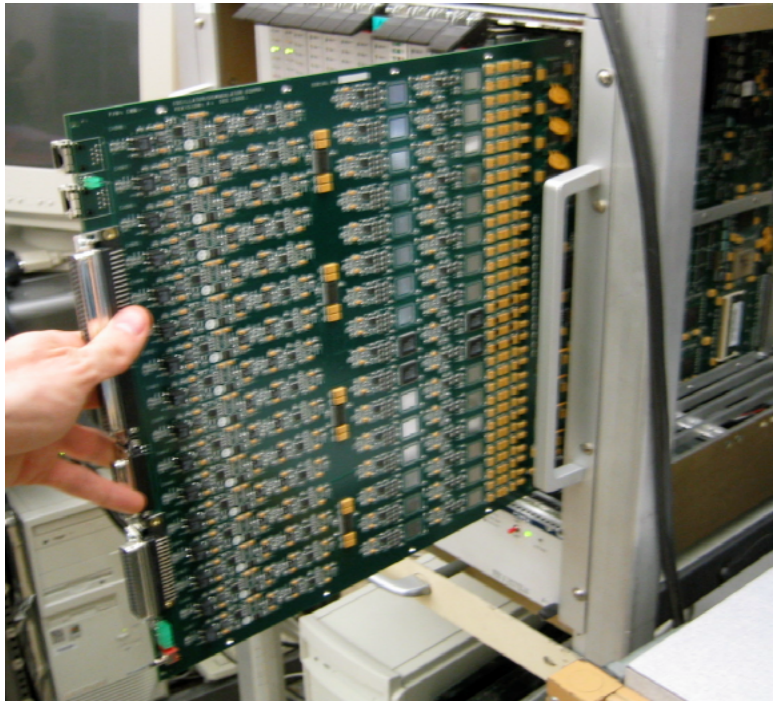

Design and prototyping at LBNL
(M. Dobbs, J. Joseph, M. Lueker, C. Vu)

Measured MUX Noise Spectrum at SQUID Amplifier Output
(Trevor Lanting)

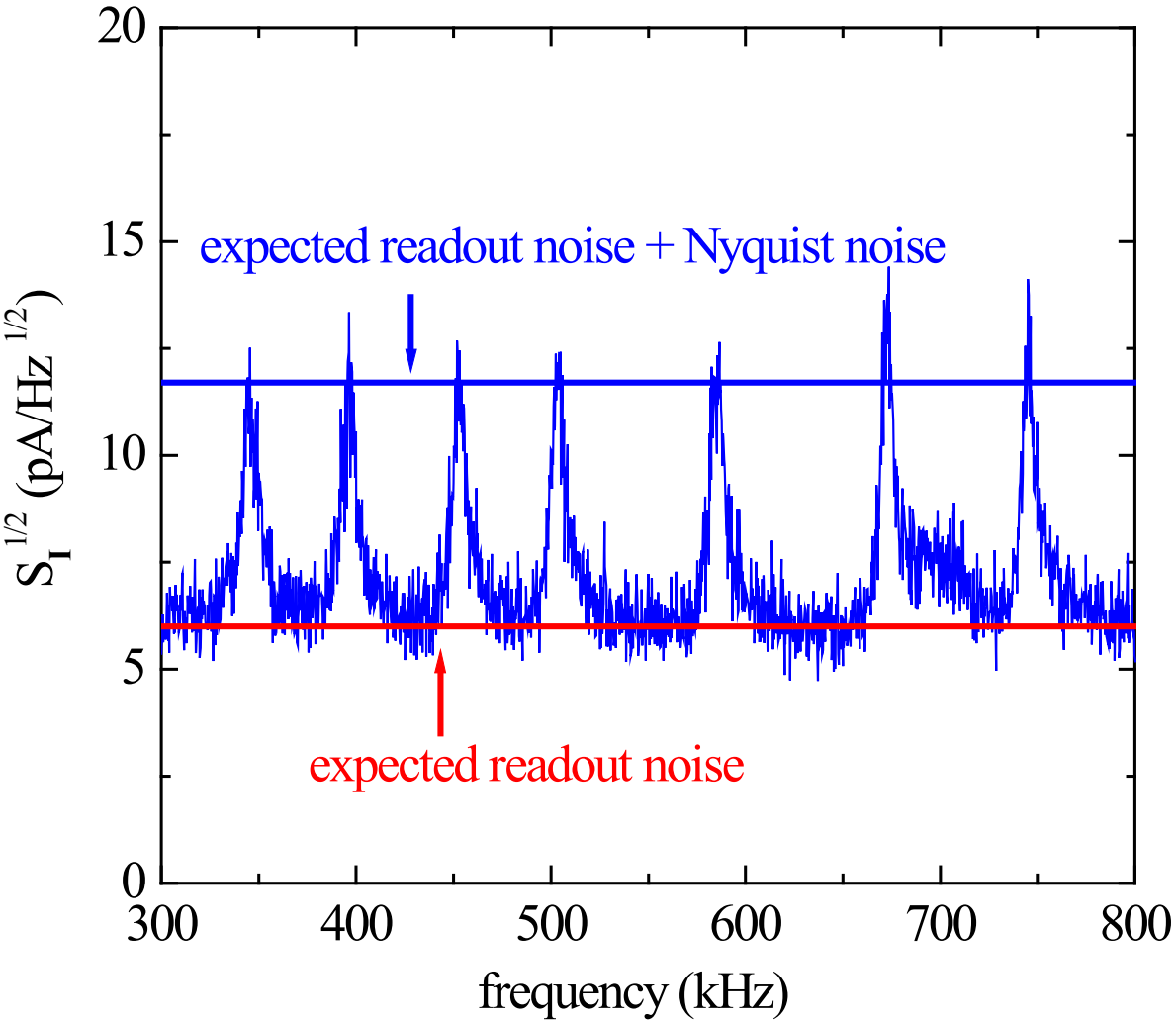

Measured Noise Spectrum in 8-Channel MUX System

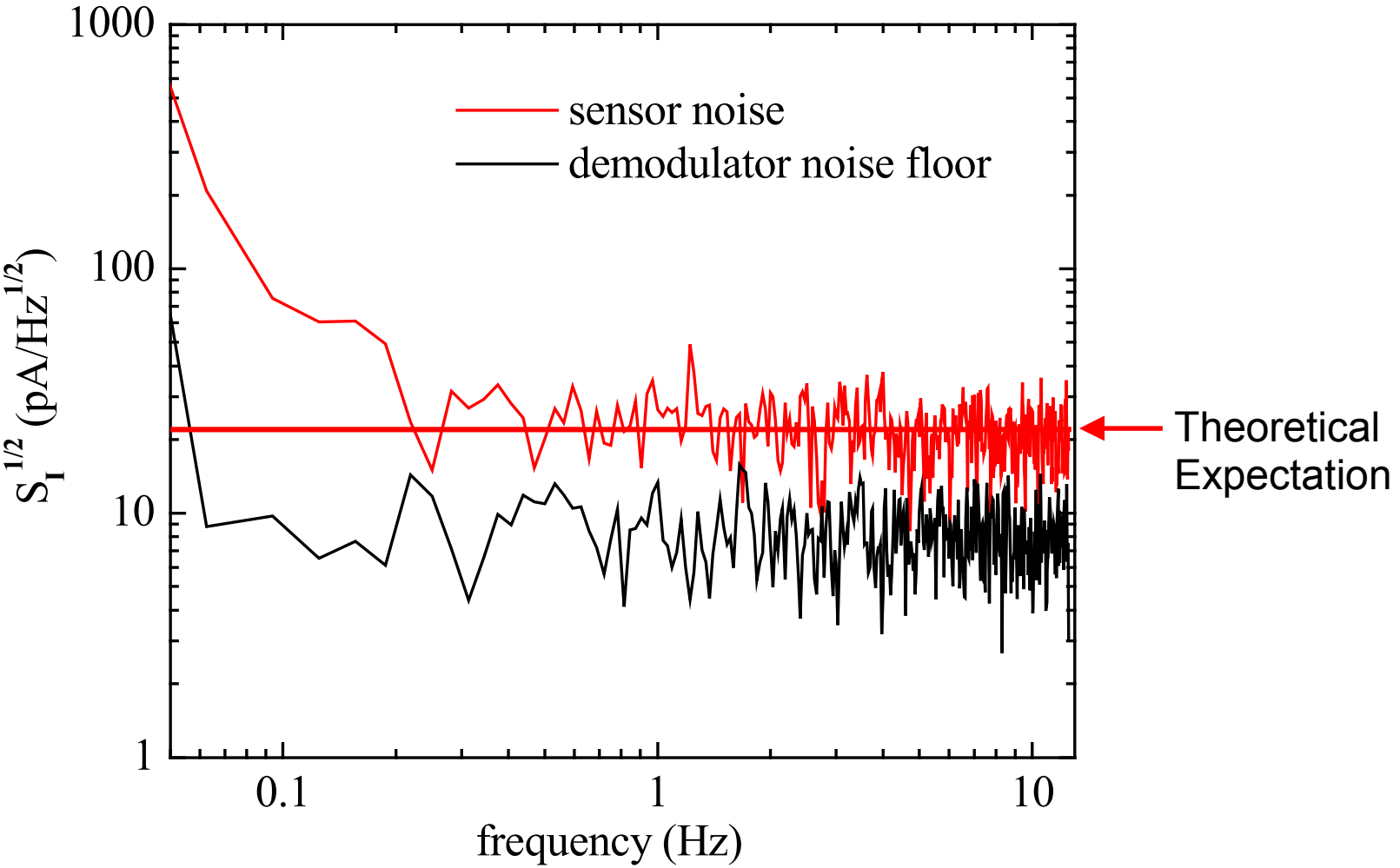

Sensor noise white above 0.2 Hz

(Trevor Lanting)

Cross-Talk < 1%

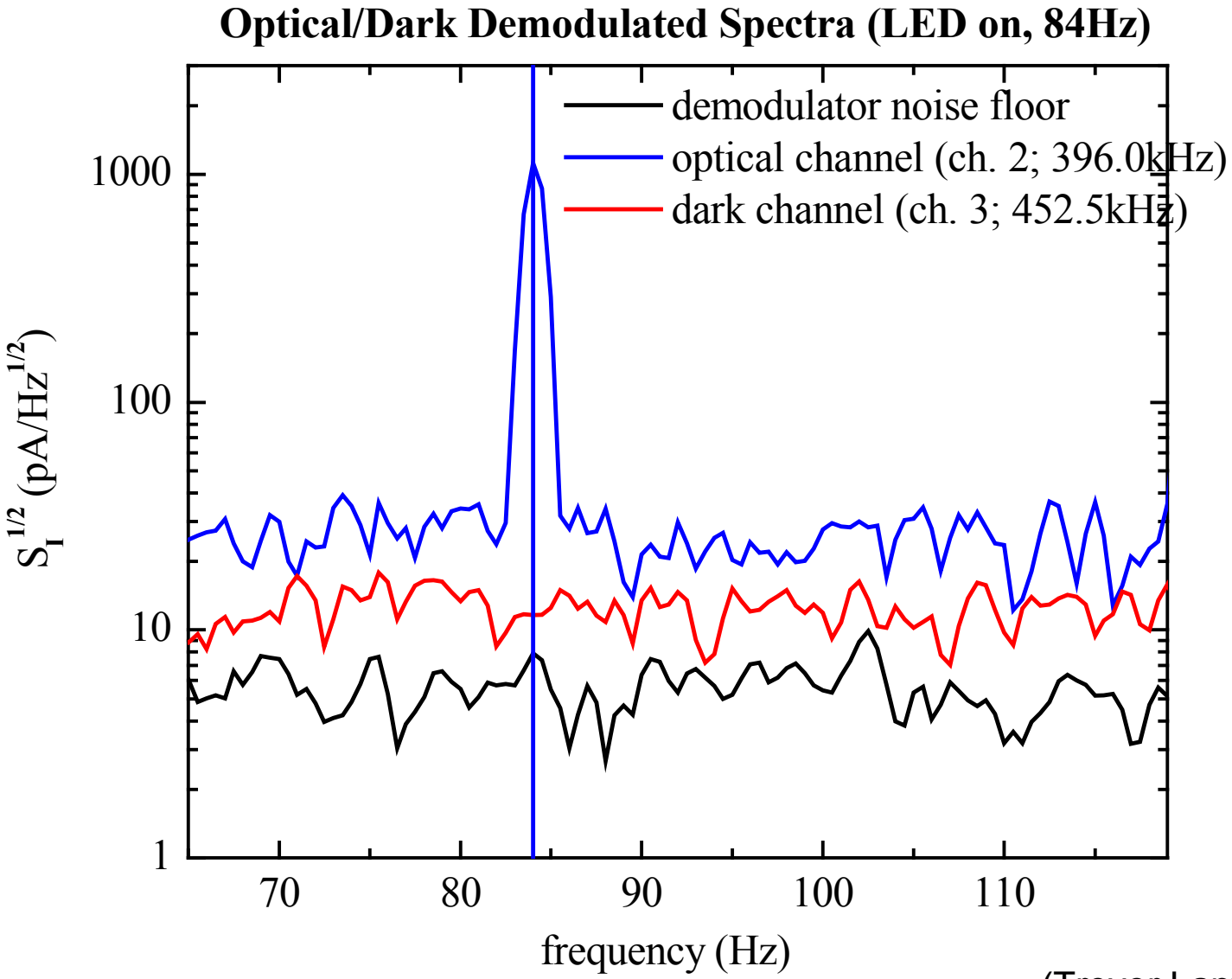

(Trevor Lanting)

MUX chip (0.25K stage)

Superconducting spiral inductors

integrated on a chip

5 mm

(fabbed by Northrup-Grumman)

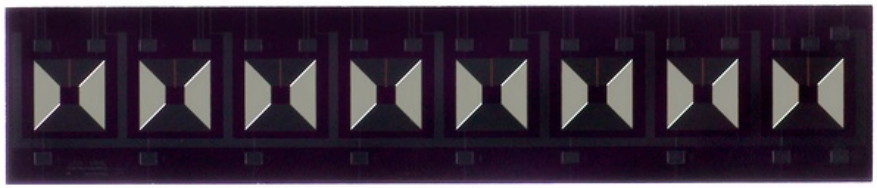

Capacitors can be integrated with inductors, but external chip capacitors require less space.

NP0 capacitors perform well at 4K

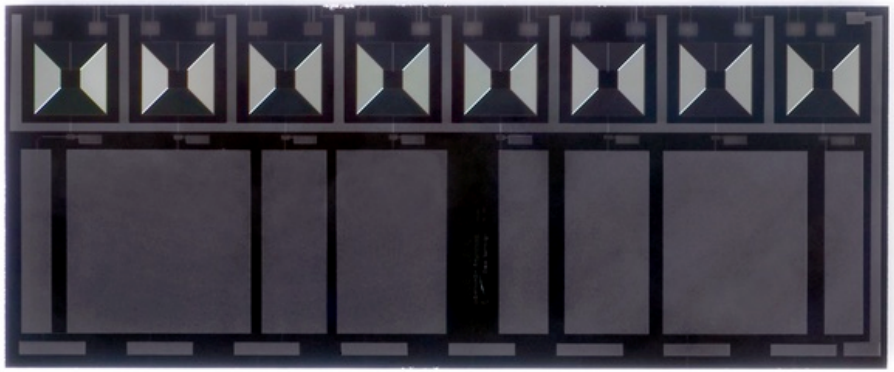

SQUIDs mounted as arrays of eight in magnetic shield (4K stage)

SQUID mounting board

SQUIDs mounted on Nb pads
to pin magnetic flux

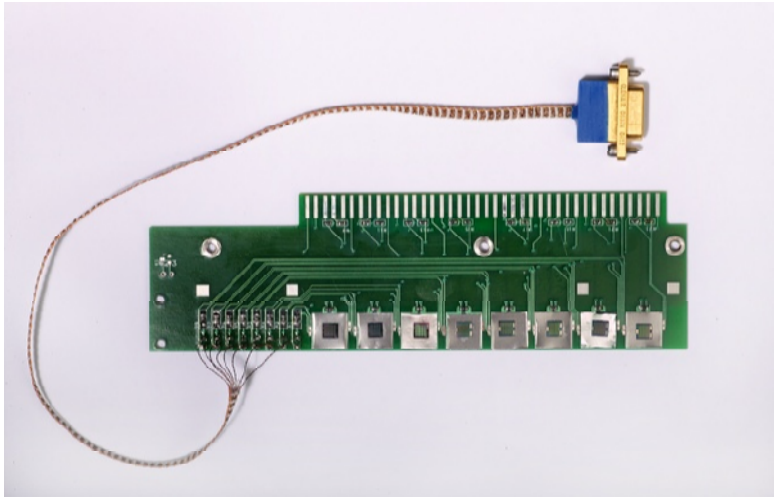

Magnetic Shield
(M. Lueker)

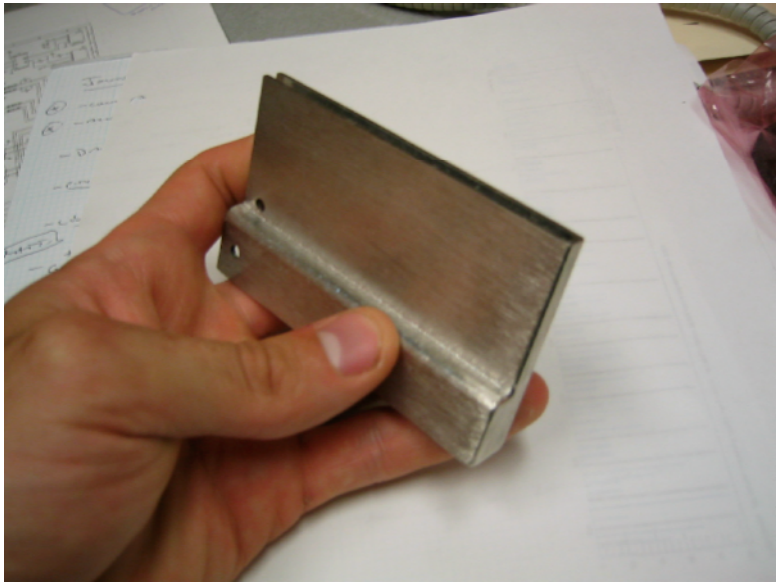

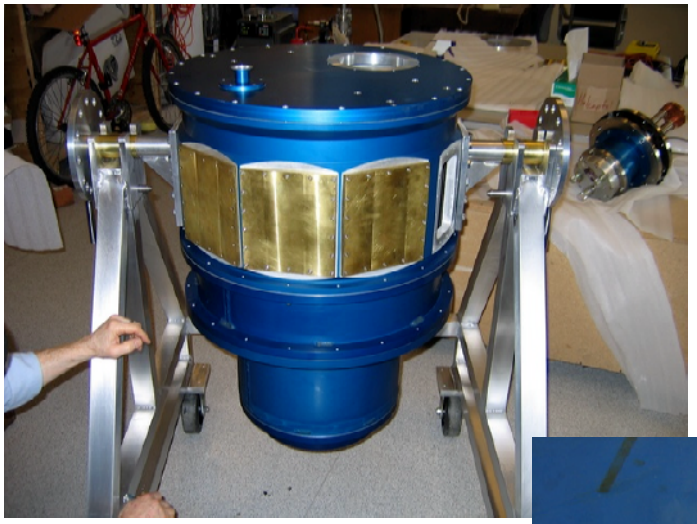

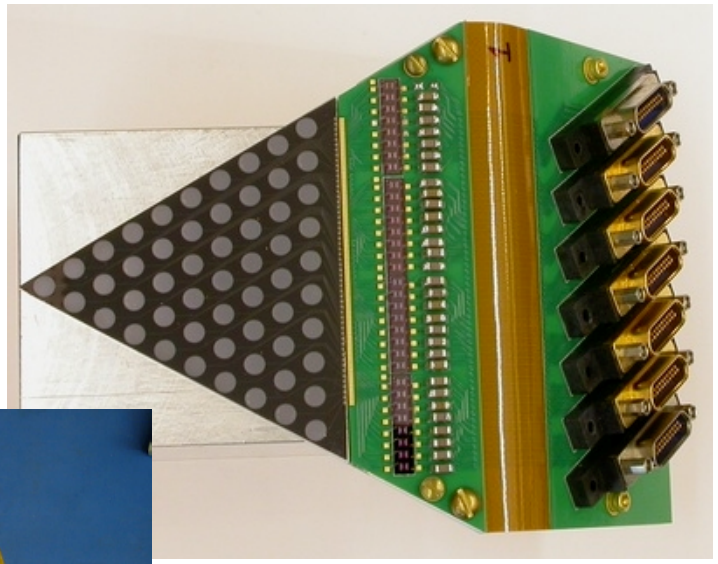

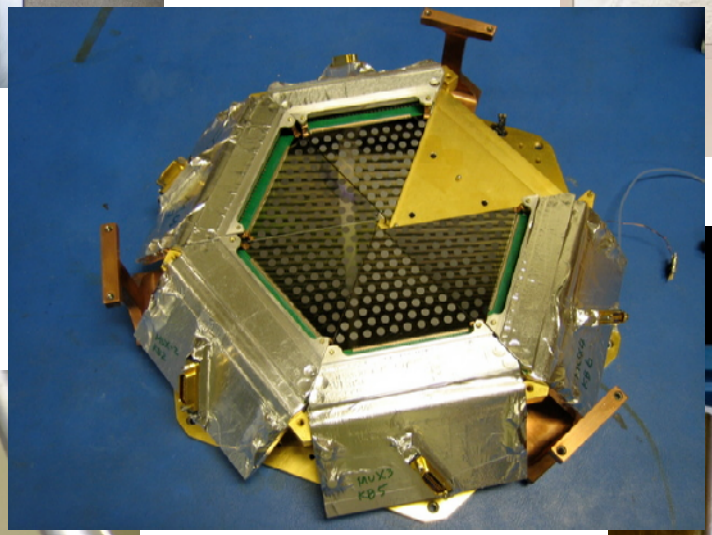

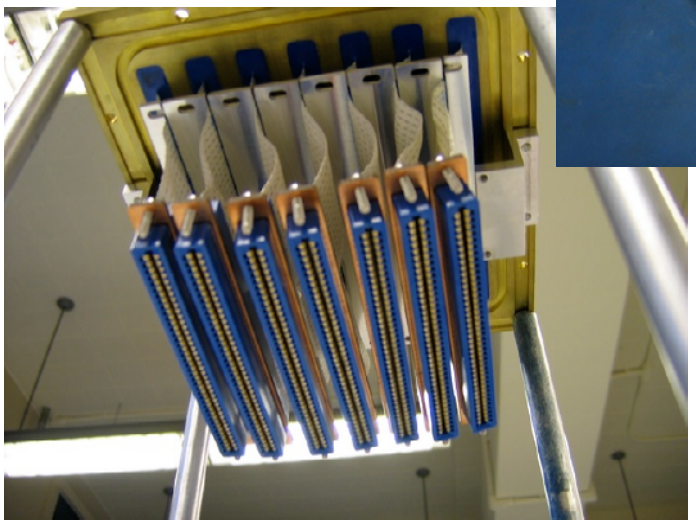

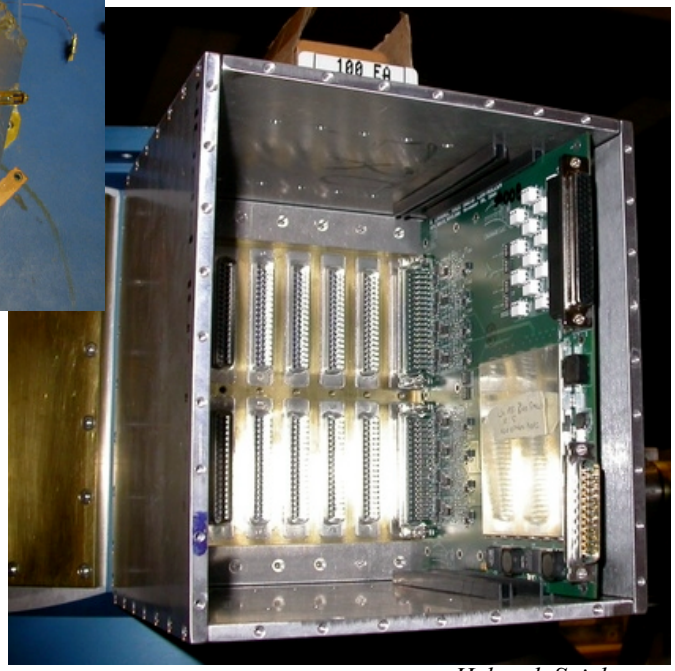

TES Array at Atacama

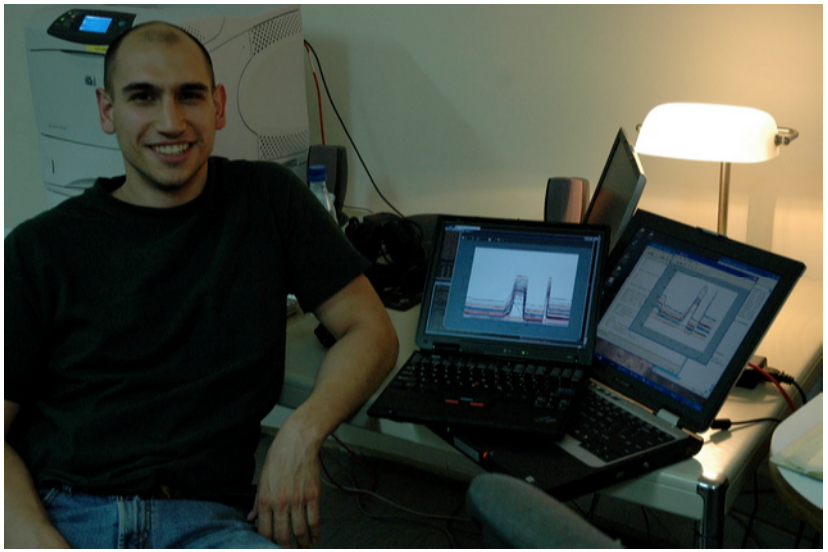

New Development: "Fully Digital" Demodulator (Matt Dobbs, LBNL/McGill)

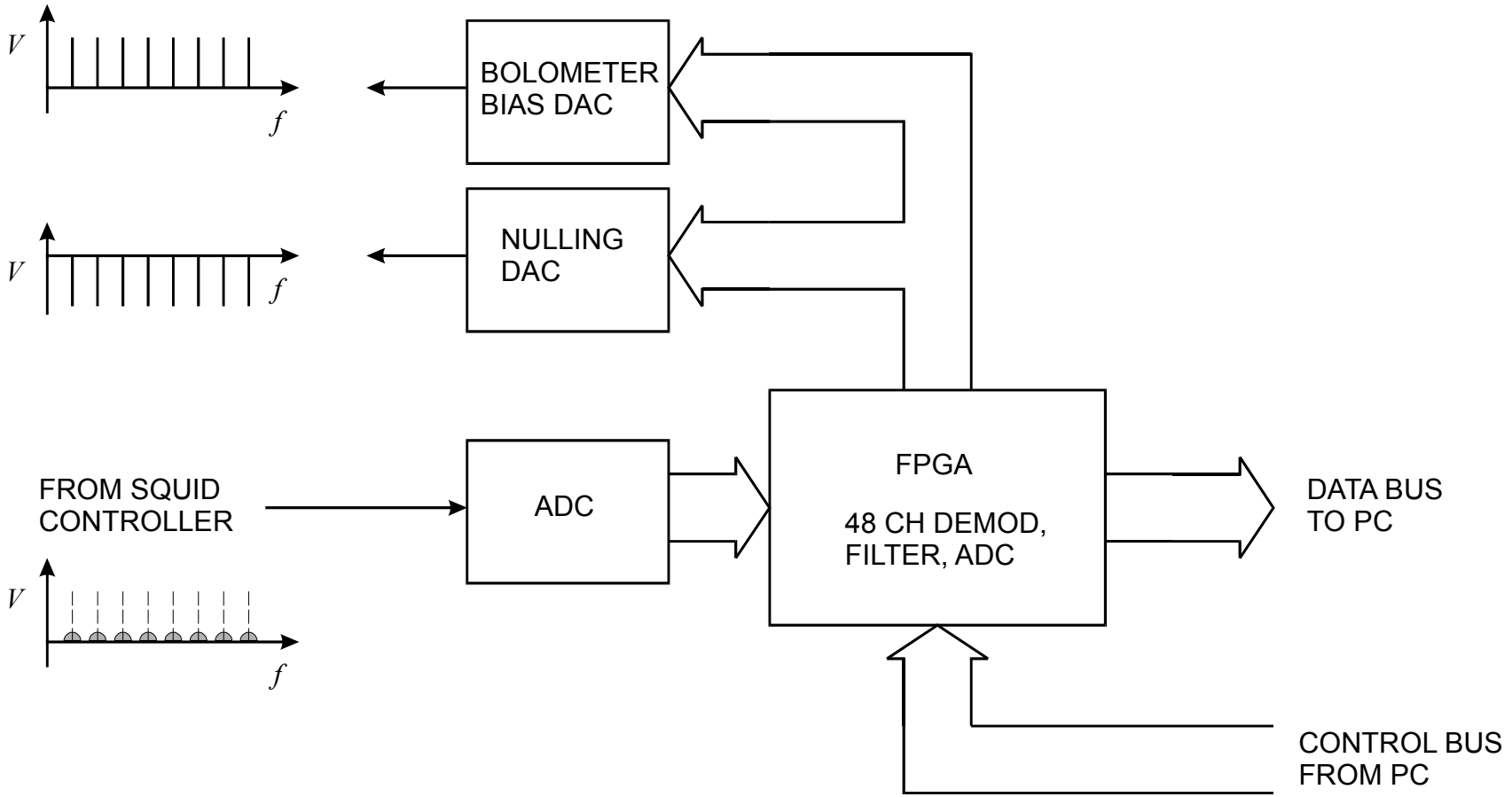

- Prototypes of key components tested
- Substantial reduction in power ⇒ Balloon-borne experiments (e.g. EBEX)
  Satellite mission (CMBPOL?)

How many bolometers can (or should) be MUXed?

Lower bounds set by

Acceptable thermal leaks in wiring (~ 300 single channels OK)

Cost (SQUIDs + wiring assemblies)

e.g. for 8-fold MUXing SQUIDs no longer major cost driver.

Upper bounds

Overall bandwidth
– determined by wiring length in SQUID feedback loop.

Single-point failure modes

Failure in a MUX module should lead to negligible loss in number of signal channels.

Baseline design for APEX-SZ and SPT: 8-fold MUXing

32-fold MUXing practical (extend max. frequency from 1 MHz to 3 MHz)

Appears adequate for 10^4 bolometers.

Technical limits to MUXing

1. Frequency spacing of bias carriers depends on selectivity of tuned circuits.

2. Minimum LC bandwidth (Q) set by bolometer time constant.

3. Channel spacing set by allowable cross-talk and noise leakage from other channels.

4. Minimum frequency set by bolometer thermal time constant
   (typ. min. 100 kHz)

5. Maximum frequency set by large-signal bandwidth of SQUID feedback loop.

   Loop gain-bandwidth product: set by
   a) required dynamic range
      (no. and magnitude of carriers)
   b) distortion in SQUID

   Limited by total wiring length of feedback loop

   Example: round trip wiring length of 20 cm limits loop gain-bandwidth product
   to ~100 MHz (at 1 MHz extend dynamic range x100)

H. Spieler, Frequency Domain Multiplexing for Large-Scale Bolometer Arrays, in Proceedings Far-IR, Sub-mm & mm Detector Technology Workshop, J. Wolf, J. Farhoomand and C. McCreight (eds.), NASA/CP-211408, 2002 and LBNL-49993, www-physics.LBL.gov/~spieler.

Solutions

1. Maximize dynamic range of SQUID

SQUID is limited by flux, so reducing the mutual input inductance allows larger input current.

Smaller input mutual inductance
increases input noise current
reduces SQUID transresistance (gain)

Limited by bolometer noise and noise of warm amplifier

$\Rightarrow$ SQUID arrays (many SQUIDs connected in series)

We use 100-SQUID arrays from NIST

2. Cold local feedback loop

Use local feedback around 300-SQUID array.
Reduced wire length increases maximum frequency.
In addition: External warm feedback loop with reduced gain-bandwidth
$\Rightarrow$ larger bandwidth for given wire length

- With SQUID array and cold/warm feedback loop ~30 channels per readout line practical.

Frequency-Domain MUX Demonstrated with Gamma-Ray Micro-Calorimeters

LLNL/UCB/LBNL collaboration

Time domain

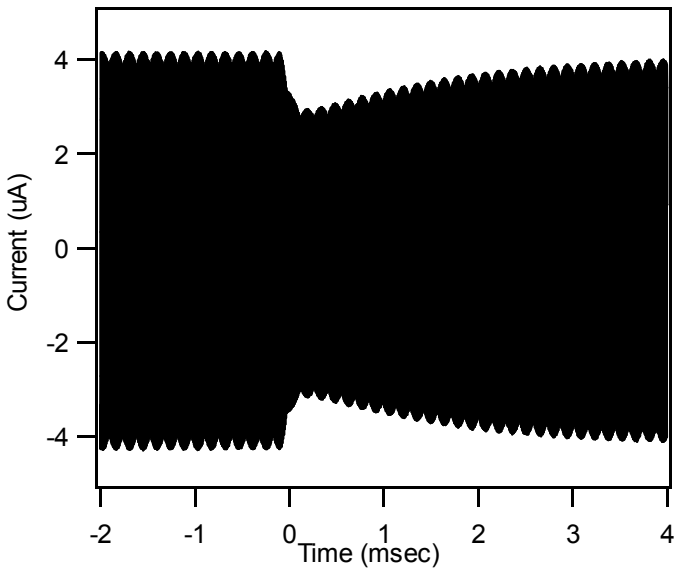

Frequency Domain

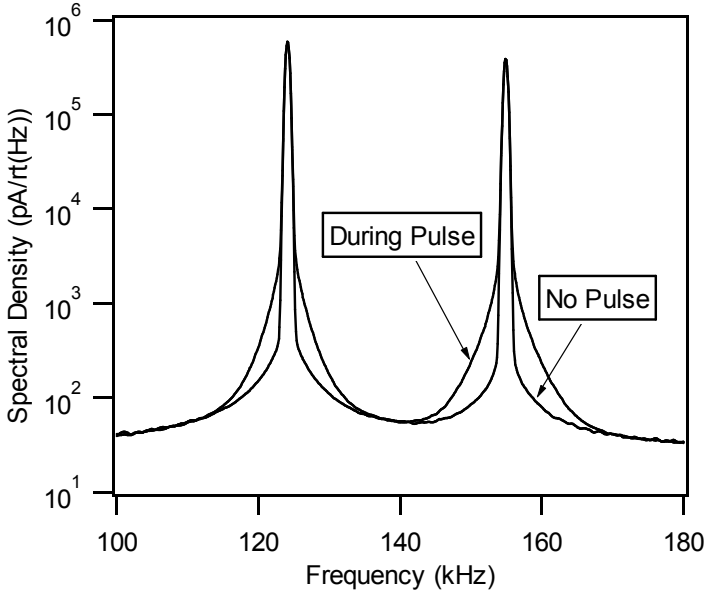

Energy resolution of 60 eV FWHM at 60 keV unaffected by multiplexer.

J. N. Ullom et al., IEEE Trans. Appl. Superconductivity **13/2** (2003) 643-648

MUXing $\Rightarrow$ increase active area, overall rate capability

Major Transition in CMB Instrumentation

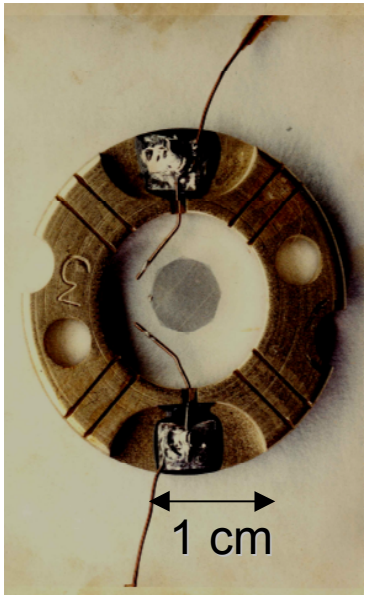

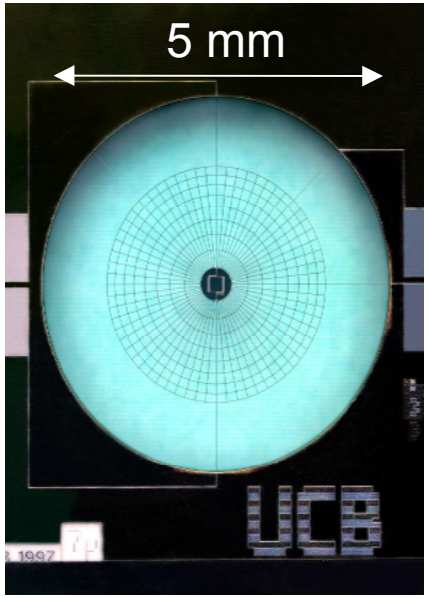

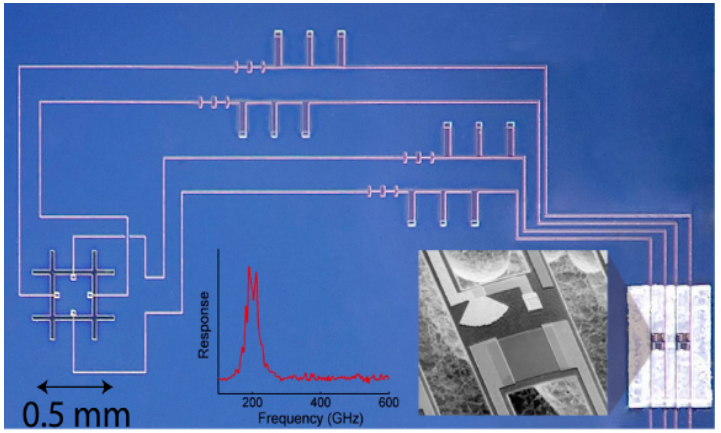

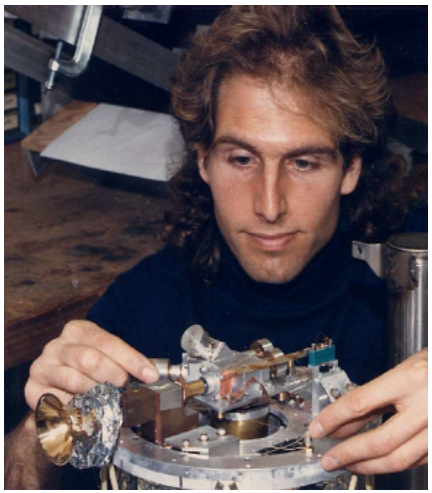

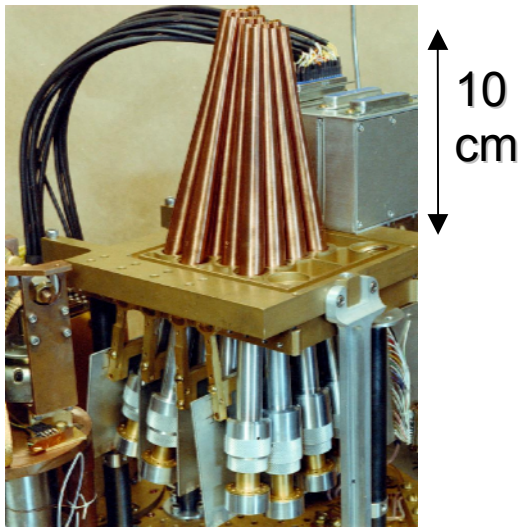

10 cm

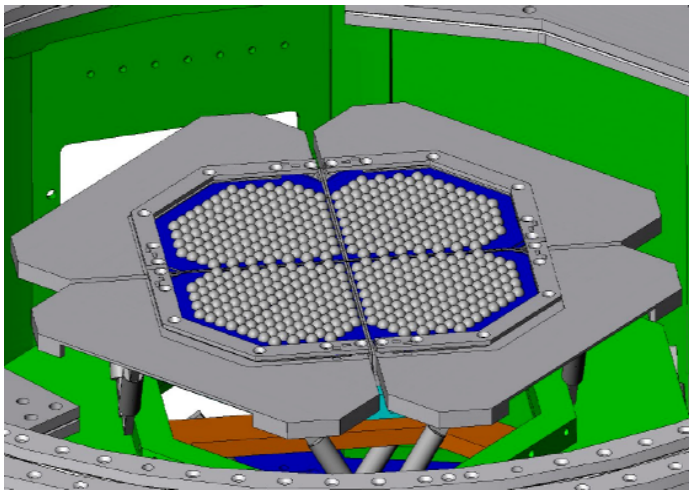

1980s 1990s 2000s

Summary

- Next-generation CMB experiments require 10^2 – 10^3 fold improved sensitivity
- Monolithic fabrication technology provides wafer-scale TES kilopixel arrays
- Antenna-coupled arrays provide polarization discrimination
- Frequency-domain MUXing demonstrated

  Zero power dissipation at 0.25K focal plane
  <1% cross-talk
  Very insensitive to vibration
  Negligible increase in noise
  Conceptually simple, but many crucial details

- System incorporates techniques from

  Cryogenics and superconductivity
  RF communications (old and new)
  Low noise analog electronics
  High Energy Physics

- Collaboration between University and National Lab essential